TECHNICAL REPORT STANDARD PAGE

1. Report No.	2. Government Accession No.	3. Recipient's Catalog No.
FHWA/LA.08/437		

4.Title and Subtitle	5.Report Date
Structural Monitoring of Rigolets Pass Bridge	October 2009
	6.Performing Organization Code

7.Author(s)	8.Performing Organization Report No.
Robert N. Bruce, Jr., John J. Roller, and Henry G. Russell	

9.Performing Organization Name and Address	10. Work Unit No.
Tulane University 6823 St. Charles Avenue New Orleans, LA 70118	11. Contract or Grant No. LTRC Project No. 04-2ST State Project No. 736-99-1215

Sponsoring Agency Name and Address	13. Type of Report and Period Covered
La Department of Transportation and Development Louisiana Transportation Research Center 4101 Gourrier Avenue Baton Rouge, LA 70808	Final Report April1, 2005 – April 30, 2009
	14.Sponsoring Agency Code

15.Supplementary Notes

Conducted in cooperation with the U.S. Department of Transportation, Federal Highway Administration

16.Abstract

The overall objective of this research project was to evaluate the structural behavior of prestressed high-performance concrete (HPC) long-span bulb-tee girders utilized in Louisiana bridge construction. To accomplish this objective, one span of the Rigolets Pass Bridge was instrumented and monitored to obtain measured strain and deflection data for a period of one year after completion of construction. Four 131-ft. (40-m) long, BT-78 girders fabricated using HPC were instrumented to measure concrete strains and deflections at midspan. During fabrication of the four instrumented girders, representative samples of the prestressing strand and HPC were obtained and used for material property studies. After fabrication, the four instrumented girders were used to construct Span 43 of the Rigolets Pass Bridge.

After erecting the instrumented girders at the bridge site, an HPC deck slab was added. During the deck slab construction for Span 43, instrumentation was added to measure concrete strains at midspan. Samples of the deck slab concrete were also obtained and used for material property studies.

Throughout the bridge construction process, instrumentation readings were taken and recorded at selected time- or event-based intervals. After completion of the Rigolets Pass Bridge construction, the strain gauge instrumentation installed in the HPC girders and deck slab of Span 43 were connected to an automated on-site data acquisition system with remote access capabilities. The on-site data acquisition system was used to record concrete temperature and strain data at selected time increments for a period of one year after completion of construction. Manual measurements of midspan deflections were taken for Span 43 at the beginning, middle, and end of the one-year bridge monitoring period.

This final report documents results from both instrumentation monitoring and material property studies performed for Span 43 of the Rigolets Pass Bridge. The results obtained from this research provide detailed information related to the long-term behavior of a long-span structure fabricated using HPC. Findings and conclusions drawn from this research can be used by the Louisiana Department of Transportation and Development (LADOTD) to develop specifications and designs for future HPC bridge structures.

17.Key Words	18.Distribution Statement
Bridges, Bulb-Tee Girders, High Performance Concrete, High-Strength Concrete, Instrumentation, Prestressed Concrete, Structural Monitoring.	Unrestricted. This document is available through the National Technical Information Service, Springfield, Va 21161

19.Security Classif.(of this report)	20.Security Classif.(of this page)	21.No. of Pages	22.Price
N/A	N/A	80	N/A

Project Review Committee

Each research project will have an advisory committee appointed by the LTRC Director. The Project Review Committee is responsible for assisting the LTRC Administrator or Manager in the development of acceptable research problem statements, requests for proposals, review of research proposals, oversight of approved research projects, and implementation of findings.

LTRC appreciates the dedication of the following Project Review Committee Members in guiding this research study to fruition.

LTRC Administrator/Manager

Walid R. Alaywan

Members

Paul Fossier	LADOTD Bridge Design
Gill Gautreau	LADOTD Bridge Maintenance
Mike Ricca	LADOTD Construction
John Eggers	LADOTD Construction
Masood Rasoulian	LADOTD Contract Services
Michael B. Boudreaux	LTRC Implementation Engineer
Arturo Aguirre	FHWA

Directorate Implementation Sponsor

William Temple

Structural Monitoring of Rigolets Pass Bridge

by

Robert N. Bruce, Jr.
Catherine and Henry Boh Chair Emeritus in Civil Engineering, Tulane University
New Orleans, LA 70118

John J. Roller
Principal Structural Engineer, CTL Group
Skokie, IL 60077

Henry G. Russell
Engineering Consultant, Henry G. Russell, Inc.
Glenview, IL 60025

LTRC Project No. 04-2ST
State Project No. 736-99-1215

conducted for

Louisiana Department of Transportation and Development
Louisiana Transportation Research Center

October 2009

ABSTRACT

The overall objective of this research project was to evaluate the structural behavior of prestressed high-performance concrete (HPC) long-span bulb-tee girders utilized in Louisiana bridge construction. To accomplish this objective, one span of the Rigolets Pass Bridge was instrumented and monitored to obtain measured strain and deflection data for a period of one year after construction. Four 131-ft. (40-m) long, BT-78 girders fabricated using HPC were instrumented to measure concrete strains and deflections at midspan. During fabrication of the four instrumented girders, representative samples of the prestressing strand and HPC were obtained and used for material property studies. After fabrication, the four instrumented girders were used to construct Span 43 of the Rigolets Pass Bridge.

After erecting the instrumented girders at the bridge site, an HPC deck slab was added. During the deck slab construction for Span 43, instrumentation was added to measure concrete strains at midspan. Samples of the deck slab concrete were also obtained and used for material property studies.

Throughout the bridge construction process, instrumentation readings were taken and recorded at selected time- or event-based intervals. After completion of the Rigolets Pass Bridge construction, the strain gauge instrumentation installed in the HPC girders and deck slab of Span 43 were connected to an automated on-site data acquisition system with remote access capabilities. The on-site data acquisition system was used to record concrete temperature and strain data at selected time increments for a period of one year after completion of construction. Manual measurements of midspan deflections were taken for Span 43 at the beginning, middle, and end of the one-year bridge monitoring period.

This final report documents results from both instrumentation monitoring and material property studies performed for Span 43 of the Rigolets Pass Bridge. The results obtained from this research provide detailed information related to the long-term behavior of a long-span structure fabricated using HPC. Findings and conclusions drawn from this research can be used by the Louisiana Department of Transportation and Development (LADOTD) to develop specifications and designs for future HPC bridge structures.

ACKNOWLEDGEMENTS

Work on this project was performed jointly by Tulane University Department of Civil and Environmental Engineering, CTLGroup, and Henry G. Russell, Inc. under the sponsorship of the Louisiana Transportation Research Center (LTRC) and in cooperation with the Louisiana Department of Transportation and Development (LADOTD). Overall design and development of project specifications for the Rigolets Pass Bridge was performed by LADOTD. Paul B. Fossier, LADOTD bridge engineer administrator, provided technical guidance throughout the project. Walid Alaywan, senior structures research engineer of LTRC, provided administrative management for the project. John Eggers, Sadi Torres, and Randy Young were responsible for the concrete materials test program and provided valuable assistance with instrumentation readings at the precasting yard and bridge site.

Appreciation is expressed to the staff of Gulf Coast Pre-Stress, Inc. of Pass Christian, MS, especially Don Theobald, for their patience during fabrication, storage, and shipping of the four instrumented girders.

Appreciation is also expressed to the staff of Massman Construction Company especially Steve Hayes and Terrence Colombatto, for their patience and assistance provided during construction of the instrumented span at the Rigolets Pass Bridge site.

IMPLEMENTATION STATEMENT

The Rigolets Pass Bridge is a 62-span bridge with a total length of 5,489 ft. (1,673 m) located on Routes US 90 and LA 433 in Orleans and St. Tammany Parishes, LA. Span lengths range from 19.7 ft. (6 m) to 254 ft. (77.5 m). HPC was incorporated in Spans 42 and 43, which comprise a continuous unit with span lengths of 131.2 ft. (40 m). The spans utilize four lines of 78-in. (1.98-m) deep precast, prestressed concrete BT-78 girders spaced at 12-ft. 7-in. (3.83-m) centers. Specified concrete compressive strength for the girders is 10,000 psi (69 MPa) at 56 days and 6,670 psi (46 MPa) at strand release.

In conjunction with the construction of the Rigolets Pass Bridge, the state of Louisiana initiated a research program with the objective of monitoring the structural behavior of one of the two HPC bridge spans. HPC Span 43 was instrumented to measure concrete strains and deflections at midspan for a period of one year after construction. Material property studies were also included in the research program. Results from this material testing and structural monitoring program provide additional information for Louisiana's growing HPC database and provide performance data related to an implementation project involving a relatively long span length. This research, along with national research efforts in this area, gave designers the information necessary to apply the new high strength concrete in the bulb-tee girder design for the I-10 twin spans. Using recommendations from this report, six lines of girders were spaced at 10 ft. 9 in. (3.28 m) rather than seven spaced at 8 ft. 10 in. (2.69 m). Furthermore, the use of high-strength, high-performance concrete allowed the BT-78 girder to span a length of 135 ft. (41 m). The BT-78 girders spanned a cumulative length of 25,920 ft. (7,900 m) in each direction. In addition, with the lower permeability associated with high performance concrete, the Louisiana Department of Transportation and Development (LADOTD) expects a minimum 75-year service life for the bridge instead of the standard 50-year service life for concrete structures.

A cost analysis was performed on the superstructure portion of the I-10 Twin Span Bridge where high-strength, high -performance bulb-tee girders were used; it was determined that a savings of about $ 16 million was realized.

The results form HPC research in Louisiana were put in the form of a design specification that is currently being used as a standard.

TABLE OF CONTENTS

LIST OF TABLES

LIST OF FIGURES

INTRODUCTION

The Louisiana Department of Transportation and Development (LADOTD) has been gradually introducing high performance concrete (HPC) into their bridge construction programs. At the same time, the Louisiana Transportation Research Center (LTRC) has been sponsoring research work to address design and construction issues related to the utilization of HPC.

In 1988, a bridge project was used as an experiment to determine if concrete with 8,000 psi (55 MPa) compressive strength could be obtained on a production product. The experiment was only partially successful because the contractor was penalized on 68 percent of the project's 2,370 ft. (723 m) of prestressed concrete girders. In 1992, a 130-ft. (39.6-m) long, square prestressed concrete pile with a compressive strength of 10,453 psi (72.1 MPa) was successfully fabricated, shipped, and driven without damage as part of the State Route 415 bridge over the Missouri Pacific Railroad. In 1993, two bridges on the Inner Loop Expressway near Shreveport were built using American Association of State Highway Transportation Officials (AASHTO) Type IV girders with a specified compressive strength of 8,500 psi (59 MPa) at an age of 28 days.

A 1994 LTRC report recommended that LADOTD consider implementation of concrete with compressive strengths up to 10,000 psi (69 MPa) in a bridge and that the bridge should be instrumented to measure long-term behavior *[1]*. This recommendation was implemented with the design and construction of the Charenton Canal Bridge, which was opened to traffic in November 1999. The successful construction of the Charenton Canal Bridge demonstrated that a HPC bridge could be designed and built in Louisiana using locally available materials.

The Charenton Canal Bridge is a 365-ft. (111.3-m) long structure made up of five 73-ft. (22.3-m) long spans, each incorporating five AASHTO Type III girders at 10 ft. (3.1 m) spacing. In conjunction with the Charenton Canal Bridge Project, a parallel research and development project was undertaken that included provisions for instrumentation and monitoring of the completed bridge and performing extensive concrete material property studies. Based on the findings from this research, it was recommended that LADOTD proceed with the implementation of HPC on all bridges where its use is deemed beneficial and economical *[2]*.

After completion of the Charenton Canal Bridge research, LADOTD considered the use of deeper, longer-spanning HPC girders incorporating 0.6-in. (15.2-mm) diameter prestressing strands on future bridge projects. To obtain test data that would provide assurance that these

girders would perform satisfactorily, a research program was conducted to evaluate the structural performance of 72-in. (1.83-m) deep bulb-tee (BT) girders made with HPC and tested under flexural fatigue, static shear, and static flexural loading conditions *[3],[4]*. Positive findings from this research paved the way for construction of the state's second bridge incorporating HPC, the Rigolets Pass Bridge.

The Rigolets Pass Bridge is a 62-span bridge with a total length of 5,489 ft. (1,673 m). HPC was used in two of the 62 bridge spans (Spans 42 and 43). These spans each utilized four 131.2-ft. (40-m) long BT-78 girders at 12-ft. 7-in. (3.83-m) spacing. In conjunction with the Rigolets Pass Bridge Project, the state initiated a research program with the objective of monitoring the structural behavior of one of the two HPC bridge spans. HPC Span 43 was instrumented to measure concrete strains and deflections at midspan until one year after completion of construction. Material property studies were also included in the research program.

OBJECTIVES

The overall objective of this research project was to evaluate the structural behavior of prestressed high-performance concrete (HPC) long-span bulb-tee girders utilized in Louisiana bridge construction. To accomplish this objective, one span of the Rigolets Pass Bridge was instrumented and monitored for the purpose of obtaining data that will be useful in the development of specifications and designs for future HPC bridge structures.

Specific objectives of the research were as follows:

1. Obtain and measure strain and deflection data from one instrumented span of the Rigolets Pass Bridge.

2. Obtain material property data for the prestressing strand and concrete used in the superstructure of the instrumented span.

3. Evaluate the measured data based on recognized analytical or design methodologies.

SCOPE

The objectives of the research were achieved with the following scope of activities:

1. Develop instrumentation, material property testing, and data collection plan.
2. Attend meetings with precast fabricator and bridge construction contractor to address research project requirements.
3. Instrument four 131.2-ft. (39.9-m) long BT-78 girders fabricated for Span 43 of the Rigolets Pass Bridge.
4. Install additional strain measurement instrumentation in the deck slab for Span 43 of the Rigolets Pass Bridge.
5. Conduct material property tests on representative samples of concrete and prestressing strand incorporated in the four instrumented girders.
6. Conduct material property tests on representative samples of the concrete incorporated in the deck slab of Span 43.
7. Measure and document concrete strains and midspan deflections at selected time- or event-based intervals.
8. Install and setup on-site automated data acquisition system with remote access capabilities.
9. Monitor the behavior of Span 43 of the Rigolets Pass Bridge for a period of one year after completion using both the data collected from the automated data acquisition system and the data from limited manual deflection measurements taken at the bridge site.
10. Analyze data.
11. Prepare final report.

METHODOLOGY

Bridge Description

The Rigolets Pass Bridge, shown in Figure 1, is a 62-span bridge with a total length of 5,489 ft. (1,673 m) located on Routes US 90 and LA 433 in Orleans and St. Tammany Parishes, Louisiana. Eighteen of the 62 bridge spans are 19.7-ft. (6-m) long slab spans used adjacent to the approach slab at each end of the bridge. The slab spans transition to a series of five or six 49.2-ft. (15-m) long spans supported by AASHTO Type II girders near each end of the bridge. The Type II girder spans transition into two series of fifteen 131.2-ft. (40-m) long spans that incorporate BT-78 girders. These thirty BT-78 spans make up approximately 70 percent of the total bridge length. The BT-78 girders transition to a 656.2-ft. (200-m) long center section comprised of a 3-span continuous girder unit with span lengths of 201, 254, and 201 ft. (61.27, 77.46, and 61.27 m).

Figure 1
Rigolets Pass Bridge

Structural design of the Rigolets Pass Bridge was in accordance with *AASHTO Standard Specifications for Highway Bridges, Sixteenth Edition*, (as amended by the current AASHTO Interim Specifications) *[5]*. The design live load for the bridge was based on the MS-18 (truck or lane) or HST-18(M) condition, whichever governed. In addition to self weight, the bridge was also designed for a future wearing surface dead load equal to 12.5 lb/ft^2 (600 N/m^2).

Construction of the Rigolets Pass Bridge was in accordance with the *Louisiana Standard Specifications for Roads and Bridges*, 2006 Edition *[6]*. The precast concrete used for most of the superstructure girders was specified to be Class "P(X)." However, two of the 62 bridge spans (Spans 42 and 43) were constructed using girders made with HPC. The HPC used in the girders of Spans 42 and 43 was specified to be Class "P(HPC)." The cast-in-place concretes used in the superstructure and substructure were specified to be Class "AA" and Class "A," respectively.

Each of the girder-supported bridge spans incorporated an 8-in. (203-mm) thick cast-in-place reinforced concrete deck slab with a specified 28-day concrete compressive strength of 4,200 psi (29 MPa). The bridge deck was designed as continuous over multiple span lengths with the main reinforcement oriented perpendicular to the direction of traffic. The main deck slab reinforcement oriented perpendicular to the traffic consisted of two layers (top and bottom) of No. 6 (19 mm) deformed, Grade 60 bars spaced 6 in. (152 mm) apart. Longitudinal reinforcement incorporated in the deck slab varied over the length and width of the span.

Fabrication of HPC Girders

HPC Spans 42 and 43 of the Rigolets Pass Bridge comprise a continuous unit with span lengths of 131.2 ft. (40 m). These spans utilize four lines of 78-in. (1.98-m) deep precast, prestressed concrete BT-78 girders spaced at 12-ft. 7-in. (3.83-m) centers, supporting an 8-in. (203-mm) thick reinforced concrete deck as shown in Figure 2. The four HPC girders used in each span were assigned specific alphanumeric designations (for example, 42A, 42B, 42C, and 42D) according to their position. The total width of the bridge deck is 45 ft. 11 in. (14 m).

All eight HPC BT-78 girders for the Rigolets Pass Bridge were fabricated by Gulf Coast Pre-Stress (GCP) located in Pass Christian, Mississippi. The HPC girders each incorporate fifty-six 0.6-in. (15.2-mm) diameter strands in the lower flange. Twelve of the 56 strands are debonded for lengths ranging from 6.6 to 39.4 ft. (2 to 12 m) at each end of the girders. Each girder also incorporates four 3/8-in. (9.5-mm) diameter strands in the upper flange.

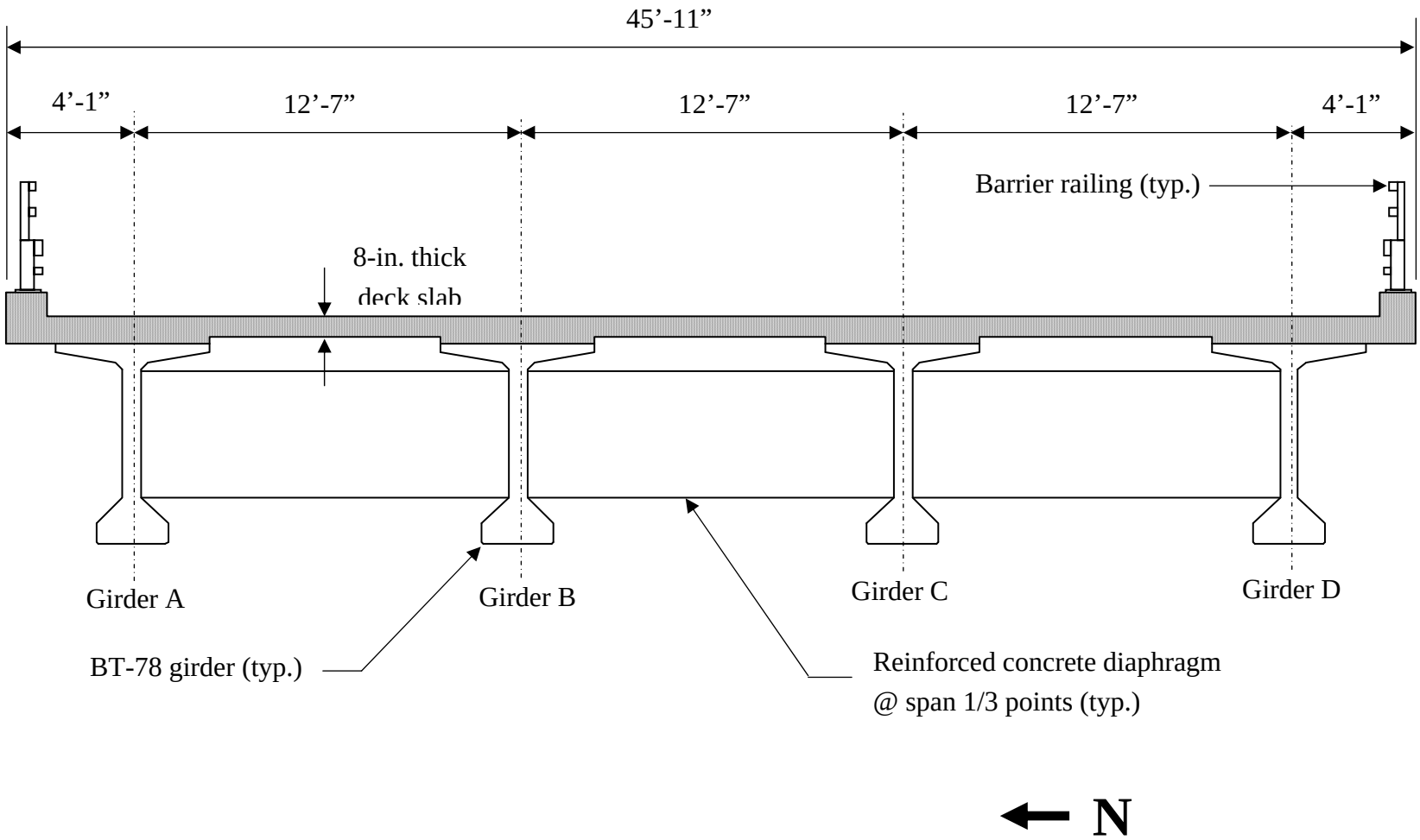

Figure 2
Cross section through HPC bridge span

All strands used in the HPC girders were specified to be low-relaxation material conforming to ASTM Designation: A416, Grade 270 (1860 MPa).

During fabrication, all strands were stressed over a bed length of 527 ft. 1-1/4 in. (160.661 m). The specified initial tension force for the 3/8-in. (9.5-mm) diameter strands in the upper flange was 10 kips (44.5 kN) or approximately 50 percent of the minimum strand breaking strength. The specified initial tension force for the 0.6-in. (15.2-mm) diameter strands in the lower flange was 43.95 kips (195.5 kN). This initial tension force corresponds with 75 percent of the specified minimum strand breaking strength.

GCP utilized a calibrated hydraulic jack to apply initial tension to the prestressing strands. Tensioning was executed by first applying a 2-kip (8.9 kN) pre-load to the strand. After applying the pre-load, tensioning continued by pulling the strand to the specified 43.95 kip (195.5 kN) initial force. The force applied to each strand was confirmed by comparing measured elongation values with a corresponding calculated value determined based on the specified force, the overall bed length between anchorage points, and an assumed strand modulus of elasticity equal to 28,800 ksi (198.6 GPa). The elongation calculation also included allowance for seating losses at each end. During the stressing of each strand, the force reading taken from the stressing unit and corresponding measured elongation value were documented by GCP on their daily production report.

After stressing all of the strands, shear and anchorage zone reinforcement was installed and secured at the required locations. Mats of mild reinforcement were also installed along the top flange of each girder. All mild reinforcement incorporated in the HPC girders was specified to conform to ASTM Designation: A615, Grade 60 (420 MPa). Once all the mild reinforcement had been secured, lifting loops were installed near each end, and the steel side forms were oiled and moved into place. After securing the side forms, the bed was ready for concrete placement.

The eight girders required for the two HPC spans (Spans 42 and 43) were fabricated using three separate castings or placements. Girders 42A, 43A, and 43B were cast on October 31, 2006. Girders 42B, 43C, and 43D were cast on November 8, 2006. Girders 42C and 42D were cast on November 14, 2006. Specified concrete compressive strengths for the HPC girders are 10,000 psi (69 MPa) at 56 days and 6,670 psi (46 MPa) at strand release. The concrete mix proportions used by GCP for fabrication of the HPC girders is shown in Table 1. The fresh concrete was transported from the batch plant and placed in the forms using standard Tuckerbuilt® concrete transport vehicles. Prior to placement, the measured slump of the concrete produced for all three castings ranged from 6-1/2 to 9 in. (165 to 229 mm).

Once placed in the forms, the concrete was consolidated using both external and internal vibrators. Each of the HPC girders required approximately 37.2 cu yd (28.5 m^3) of concrete.

Table 1
Mix proportions for HPC girders

Material	Quantities	
	per yd^3	per m^3
Portland Cement Type III	846 lb.	502 kg
Silica Fume	100 lb.	59 kg
Fine Aggregate	1,149 lb.	682 kg
Course Aggregate−Limestone	1,866 lb.	1,107 kg
Water	204 lb.	121 kg
Water Reducer, ASTM C494−Type D	38 fl oz.	1,470 ml
High-Range Water Reducer, ASTM C494–Type F	51 fl oz.	1,973 ml
Air Entrainment	None	None
Water/Cementitious Materials Ratio	0.22	0.22

Immediately after placing the concrete, the bed was covered with a tarpaulin that remained in place until the required release strength was achieved. None of the HPC girders for the Rigolets Pass Bridge required steam curing. During the initial curing period, GCP monitored concrete temperatures at the middle and both ends of the casting bed. Concrete temperatures measured during the initial curing period in the bottom flange of a girder near midspan for two of the three HPC placements are shown in Figure 3. Based on the data in Figure 3, the concrete in the bottom flange near midspan achieved a maximum temperature of approximately 153º F (67ºC) for both castings. The maximum temperature was achieved approximately 12 hours after completion of the placement and then started to decrease at a rate of approximately 3º F (1.5ºC) per hour.

GCP produced several match-cured cylinders during the three HPC girder castings. These cylinders were made in 4 x 8-in. (102 x 203-mm) molds and were cured to match the temperature measured in the girder lower flange region. The match curing regime began immediately after placement and continued until a cylinder test indicated that the required release strength had been achieved. After initial curing, the cylinders were stripped and cured under ambient conditions in the plant until tested. Results from all compressive strength tests performed by GCP on match-cured cylinders that they produced for the three HPC castings are shown in Table 2. As indicated by the data in Table 2, the required release strength of 6,670 psi (46 MPa) was typically achieved within 15 hours after completion of the cast.

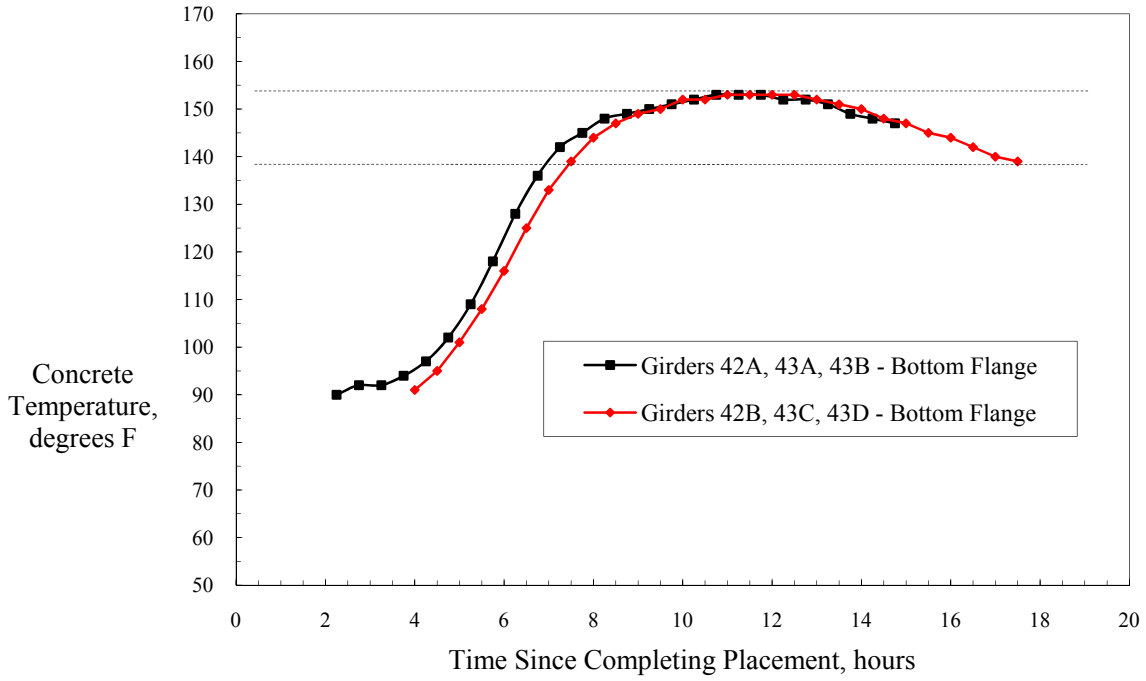

Figure 3
Initial curing temperatures measured by GCP at midspan

Table 2
HPC compressive strength results measured by GCP

Concrete Age	Concrete compressive strength					
	Pour 42A, 43A, 43B		Pour 42B, 43C, 43D		Pour 42C, 42D	
	psi	MPa	psi	MPa	psi	MPa
Release	7,570[a]	52	8,840[b]	61	9,180[a]	63
	—	—	9,010[b]	62	8,610[a]	59
14 days	9,000	62	—	—	—	—
	10,620	73	—	—	—	—
28 days	10,840	75	10,770	74	10,130	70
	10,630	73	10,850	75	10,140	70
	10,390	72	11,200	77	10,660	74

a Release strength measured at an age of 15 hours.
b Release strength measured at an age of 17.5 hours.
— Test not performed at designated age.

After achieving the required release strength, the tarpaulin used to cover the bed and the steel side forms were removed. Release of the prestressing strands then commenced, following the detensioning sequence shown on the GCP girder fabrication drawings. After release of the strands, the girders were moved into storage until needed at the bridge site.

Instrumentation of HPC Bridge Span

In conjunction with the construction of the Rigolets Pass Bridge, the state initiated a research program with the objective of monitoring the structural behavior of one of the two HPC bridge spans. The four HPC BT-78 girders and the deck slab for Span 43 of the Rigolets Pass Bridge were instrumented to monitor prestressing forces, concrete strains, and deflections. Details associated with each type of instrumentation were as follows.

Prestressing Forces

During fabrication of the BT-78 girders for Span 43, six of the 54 prestressing strands were instrumented with load cells to measure strand force levels beginning at the time of initial tensioning and continuing until release. Prior to stressing, load cells were installed on selected strands at the dead end (anchorage end) of the bed. The specific strands that were instrumented with load cells are indicated in Figure 4. Individual load cell readings were made before stressing (zero reading), after stressing the instrumented strand, after stressing all strands, prior to concrete placement, after concrete placement, prior to strand release, and after strand release (return to zero load). Additional interim load cell readings were taken at selected time-based intervals.

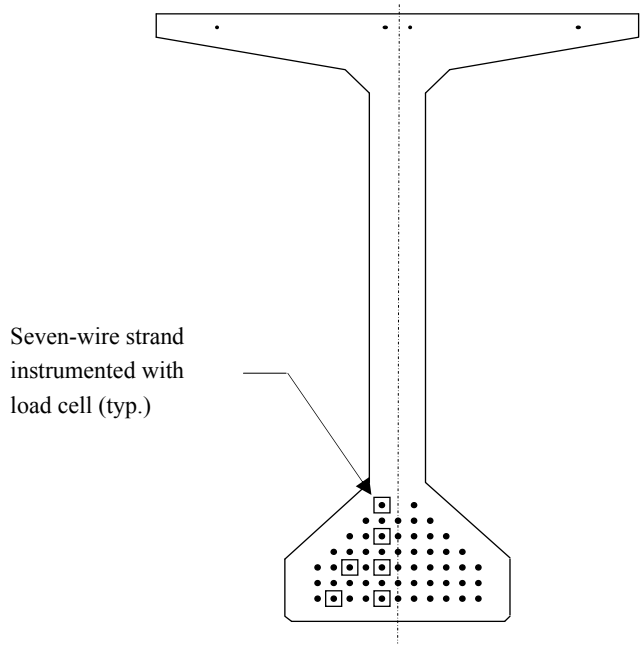

Figure 4
Load cells installed on selected prestressing strands

Concrete Strains

Five vibrating wire strain gages (VWSGs) were installed at midspan of each of the four instrumented girders to monitor concrete strains and prestress losses. Each VWSG incorporated a thermistor for measuring the concrete temperature associated with each strain measurement. As indicated in Figure 5, three of the VWSGs were installed in the lower flange at the elevation of the strand group centroid. The remaining two gages were installed at the center of gravity of the top flange located approximately 3 in. (76 mm) down from the top surface of the girder. During construction, readings for the VWSGs installed in each girder were taken after installation, prior to concrete placement, after concrete placement, prior to strand release, after strand release, after girder storage, at a concrete age of 28 days, once a month for the next two months, before shipping, after erection, and before and after casting the deck slab concrete.

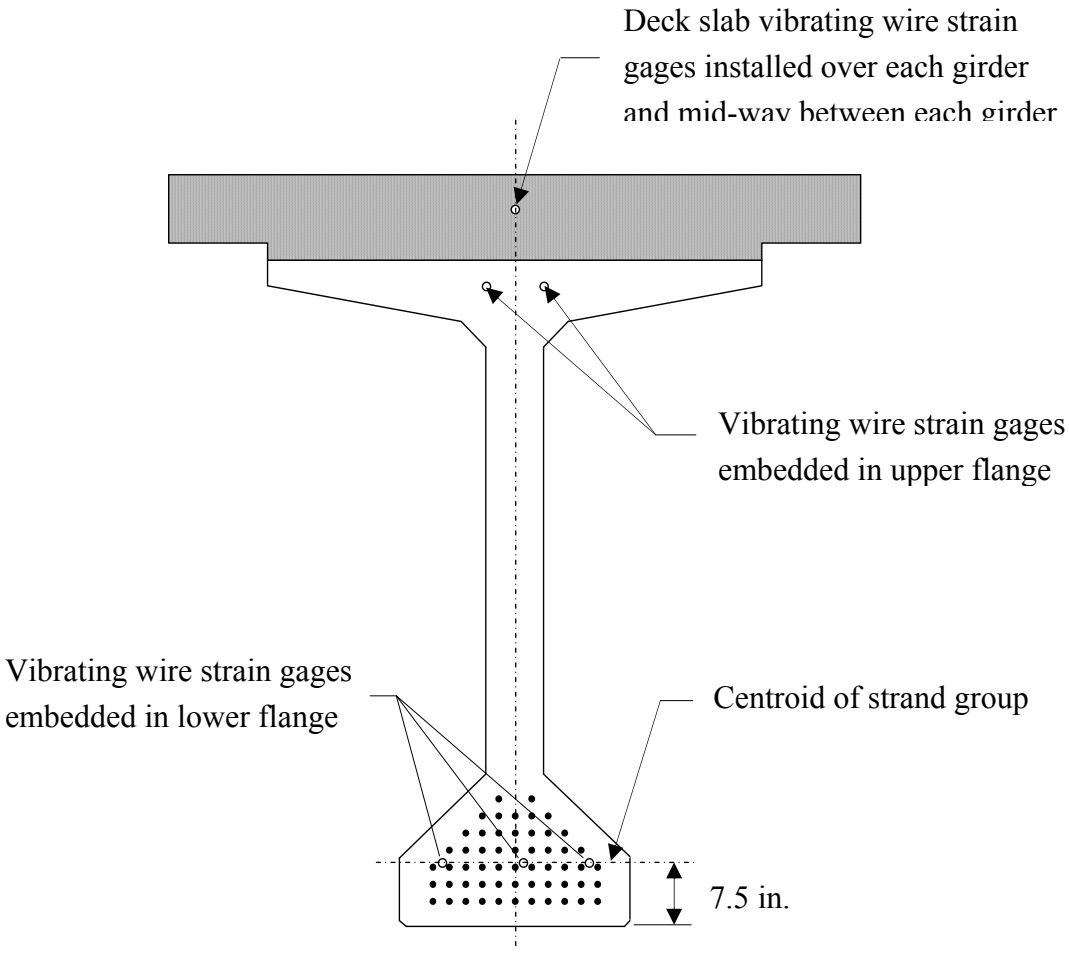

Figure 5
Vibrating wire strain gage instrumentation

Seven additional VWSGs were installed in the deck slab of Span 43 at midspan. As indicated in Figure 5, the VWSGs in the deck slab were installed directly above each girder and at the mid-point between each of the four girders. All seven of these VWSGs were installed at mid-depth in the 8-in. (203-mm) thick deck slab. During construction, readings for the VWSGs installed in the deck slab were taken after installation and before and after casting the deck slab concrete.

After casting the deck slab concrete, readings for all the VWSGs installed in both the girders and deck slab were taken once a week for the first month and once a month until the on-site data acquisition system (DAS) was installed.

Girder Deflections

Three elevation reference points were embedded along the top flange of each of the four instrumented girders. These points were embedded at midspan and near both ends to provide a permanent reference for girder deflection measurements. Each reference point consisted of a threaded steel stud with a machined indentation at one end. Each point was embedded with the indentation end protruding from the concrete surface approximately 1 in. Acorn capping nuts were threaded on the protruding end of each stud to protect the machined indentation from weather. A photograph of a typical reference point is shown in Figure 6.

Figure 6
Typical elevation reference point

Girder deflection measurements required the use of a standard surveyor's level and tripod. However, the custom steel rod used for the measurements incorporated a machined conical point at one end to interface with the indentation on the top of each elevation reference point, a stainless steel ruler with smallest measurement divisions of 1/16 in. (1.6 mm), and a reference plumb bubble. Deflection measurements were made using the level to sight elevations at each reference point location. Based on these measurements, the deflection was calculated by subtracting the average elevation of the two girder ends from the midspan elevation.

During construction, girder midspan deflection measurements were made prior to strand release, after strand release, after girder storage, at a concrete age of 28 days, once a month for the next two months, before shipping, after erection, and before and after deck casting. Prior to casting the deck slab, the elevation reference points embedded in the top surface of each girder were extended to the elevation of the finished surface of the deck slab. After casting the deck slab, deflection measurements were made once a week for the first month, once a month for the first three months, and every 6 months during the one-year monitoring period.

On-Site Automated Data Acquisition System

During construction of Span 43, the lead wires for the twenty-seven embedded VWSGs were routed to the south side where they exited the side of the deck slab at a common location near midspan. From the point of exit, the lead wires were routed in a single conduit to a large enclosure box mounted on the south barrier railing. Provisions for providing 120V electrical power and telephone service at the enclosure box were made by the bridge construction contractor. After construction of the instrumented bridge span had been completed, an on-site DAS with remote access and data collection capabilities was installed within the enclosure. After installation, the VWSGs were connected to the DAS, communications were established, and the system was programmed to collect data at established time increments.

After completion of the Rigolets Pass Bridge, data from VWSGs installed in the girders and deck slab was recorded over a one -year monitoring period. During this period, data from all VWSGs were read and stored once per hour. Stored data was downloaded via remote telephone modem access once a week and checked against previously stored data to ensure that the system was functioning properly.

Material Property Testing Program

Prestressing Strand

During fabrication of the four instrumented girders, representative samples of 0.6-in. (15.2-mm) diameter prestressing strands were taken for material property tests. One 5-ft. (1.52-m) long sample was taken from each of the seven coils of strands used. The strand samples were tested to determine breaking strength, 1 percent elongation load (yield), modulus of elasticity, and total elongation.

Girder Concrete

Material property tests were performed on specimens representing concrete placed in the midspan region of each of the four instrumented girders. Concrete compressive strength (ASTM C 39), modulus of elasticity, (ASTM C 469), unit weight, modulus of rupture (ASTM C 78), coefficient of thermal expansion (CRD C-39), creep and shrinkage (ASTM C 512), and permeability (ASTM C 1202) tests were performed according to the schedule shown in Table 3. Concrete cylinders used for compressive strength and modulus of elasticity tests were "match-cured" to match the temperature in the lower flange of each corresponding girder. Other "field-cured" specimens were covered with plastic and stored on tables situated adjacent to the casting bed. Just prior to release of the strands, all of the match- and field-cured specimens were stripped from the molds. The field-cured specimens required for coefficient of thermal expansion, creep, and shrinkage tests scheduled to commence at an age of three days were shipped to CTL Group. All other specimens were transported to LTRC for storage and future testing.

Deck Slab Concrete

Material property tests were performed on specimens representing the concrete placed in the midspan region of Span 43. Concrete compressive strength (ASTM C 39), modulus of elasticity (ASTM C 469), unit weight, modulus of rupture (ASTM C78), coefficient of thermal expansion (CRD C-39), and permeability (ASTM C1202) tests were performed in accordance to the schedule shown in Table 4. All of the specimens required for the deck slab concrete test program were initially field-cured at the bridge site. The specimens required for coefficient of thermal expansion tests scheduled to commence at an age of three days were shipped to CTLGroup the day after the deck slab was poured. All other specimens were transported to LTRC for storage and future testing.

Table 3

Girder concrete testing program

Girder	Compressive strength and modulus of elasticity test specimens (4 x 8-in. cylinder)					Modulus of rupture test specimens (6 x 6 x 20-in. beam)		Permeability test specimens (6 x 12-in. cylinder)		Coefficient of thermal expansion test specimens (6 x12-in. cylinder)			Creep and shrinkage test specimens (6 x 12-in. cylinder)		
	Initial curing method	Test age, days				Initial curing method	Test age, days	Initial curing method	Test age, days	Initial curing method	Test age, days		Initial curing method	Test age, days	
		R	28	56	90		56		56		3	90		3	90
43A	Match	3	3	3	3	Field	3	Field	3	Field	—	—	Field	—	—
43B	Match	3	3	3	3	Field	3	Field	3	Field	—	—	Field	—	—
43C	Match	3	3	3	3	Field	3	Field	3	Field	—	—	Field	—	—
43D	Match	3	3	3	3	Field	3	Field	3	Field	3	3	Field	3	3

— *Test not performed at designated age.*

Table 4
Deck slab concrete testing program

Material property	Specimens assigned for each test age				
	3 days	7 days	28 days	56 days	90 days
Compressive strength and modulus of elasticity test specimens (4 x 8-in. cylinder)	—	3	3	—	3
Modulus of rupture test specimens (6 x 6 x 20-in. beam)	—	—	3	3	—
Permeability test specimens (6 x 12-in. cylinder)	—	—	—	3	—
Coefficient of thermal expansion test specimens (6 x 12-in. cylinder)	3	—	—	—	3

— *Test not performed at designated age.*

DISCUSSION OF RESULTS

Girder Concrete Material Properties

Measurements of compressive strength, modulus of elasticity, modulus of rupture, chloride permeability, coefficient of thermal expansion, creep, and shrinkage were made on test specimens representing concrete placed in the midspan region of the instrumented girders. Measured concrete properties, except creep and shrinkage, are presented in Table 5.

Concrete compressive strength tests were performed in accordance with ASTM C 39 at four different test ages. Average measured concrete compressive strength values for the four instrumented girders determined from tests of match-cured cylinders are shown in Figure 7. Based on previous research, it was determined that match-cured cylinders yielded higher measured concrete compressive strengths at all ages than field-cured cylinders *[2]*. Therefore, for this research, only match-cured cylinders were used to determine girder concrete compressive strength and modulus of elasticity properties. As indicated by the data presented in Figure 7, the concrete used in the four instrumented girders exhibited very similar compressive strength values at all test ages.

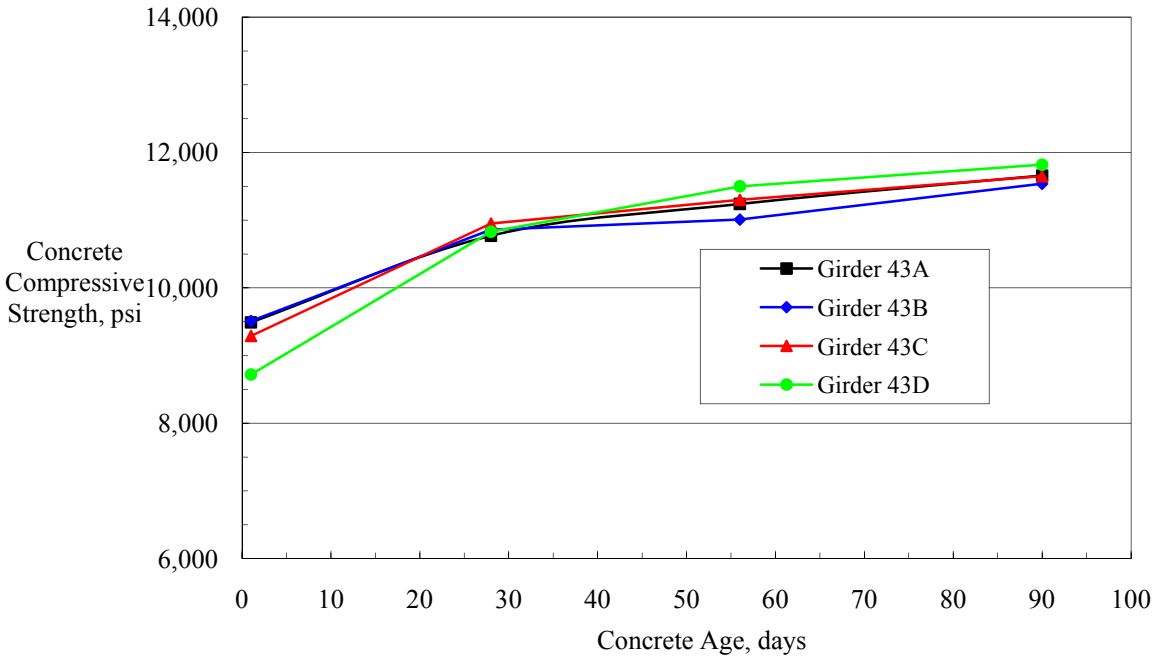

Figure 7
Average concrete compressive strength versus age

Table 5
Girder concrete material properties

Material Property	Specimen Size	Initial Curing	Girder	Concrete Age			
				Release	28 days	56 days	90 days
Compressive Strength,[a] psi	4 x 8-in. cyl.	Match	43A	9,490	10,770	11,240	11,660
			43B	9,510	10,860	11,010	11,540
			43C	9,290	10,950	11,300	11,650
			43D	8,720	10,830	11,500	11,820
			Average	9,253	10,853	11,263	11,668
Modulus of Elasticity,[a] ksi	4 x 8-in. cyl.	Match	43A	6,300	6,250	6,350	6,400
			43B	6,050	6,050	6,150	6,250
			43C	5,950	6,150	6,200	6,650
			43D	5,700	5,850	6,450	6,600
			Average	6,000	6,075	6,288	6,475
Unit Weight,[a] lb./ft^3	4 x 8-in. cyl.	Match	43A	146.8	146.1	146.9	147.3
			43B	147.1	146.1	145.3	147.4
			43C	146.4	146.2	146.1	145.5
			43D	146.0	146.3	145.6	146.0
			Average	146.6	146.2	146.0	146.6
Modulus of Rupture,[a] psi	6 x 6 x 20-in. beam	Field	43A	—	—	940	—
			43B	—	—	1,010	—
			43C	—	—	1,070	—
			43D	—	—	940	—
			Average	—	—	990	—
Permeability,[a] Coulombs	6 x 12-in. cyl.	Field	43A	—	—	136	—
			43B	—	—	140	—
			43C	—	—	156	—
			43D	—	—	170	—
			Average	—	—	151	—
Coefficient of Thermal Expansion,[b] millionths/ºF	6 x 12-in. cyl.	Field	43D - 1	—	4.58	—	5.70
			43D - 2	—	4.30	—	5.18
			43D - 3	—	4.47	—	5.75
			Average	—	4.45	—	5.54
			Overall Average = 5.00				

a *Each reported test value represents the average for three individual tests. Average values represent results from twelve individual tests.*

b *Each reported test value represents one individual test. Reported release values were measured at a concrete age of 28 days instead of the planned 3- day test.*

— *Test not performed at designated age.*

The specified concrete compressive strength for the HPC girders is 10,000 psi (69 MPa) at 56 days and 6,670 psi (46 MPa) at release. As indicated by the data reported in Table 5 and Figure 7, the measured concrete compressive strengths for girders 43A, 43B, 43C, and 43D exceeded the specified strength at both the release and 56-day test ages.

Modulus of Elasticity

Concrete modulus of elasticity tests were performed in accordance with ASTM C 469 at four different test ages. Concrete modulus of elasticity versus compressive strength data for the four instrumented girders is presented in Figure 8. For the purpose of comparison, measured data obtained from other previous HPC research sponsored by LTRC is also shown in Figure 8 *[1]*, *[2]*, *[3]*. The solid line shown in Figure 8 represents the relationship between concrete compressive strength and modulus of elasticity given by the $E_c = w_c^{1.5}\, 33\sqrt{f'_c}$ expression from Article 8.7.1 of the *AASHTO Standard Specifications for Highway Bridges*, where w_c is taken as 145 pcf (2,323 kg/m3) *[5]*. As indicated by the data presented in Figure 8, the AASHTO standard specification relationship between compressive strength and modulus of elasticity appears to be reasonably consistent with the measured data for strength levels up to 10,000 psi (69 MPa). However, correlation between the AASHTO expression and the measured data appears to diminish somewhat for higher compressive strength levels.

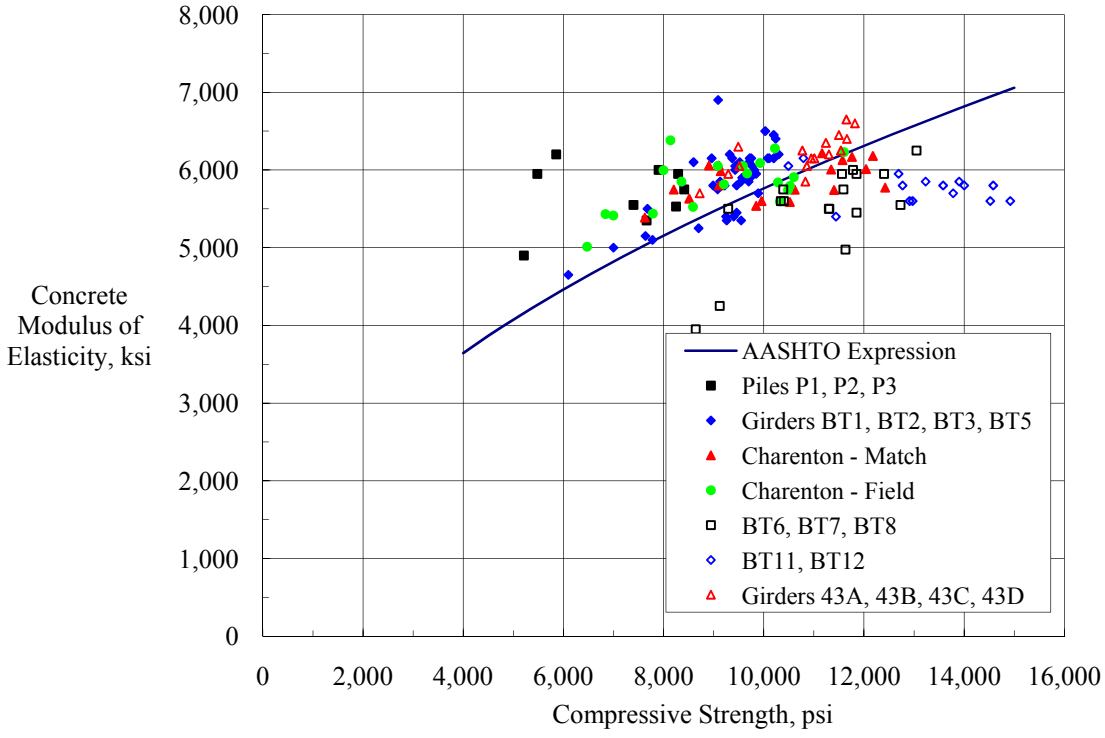

Figure 8

Concrete modulus of elasticity versus compressive strength

As indicated by the data presented in Figure 8, the AASHTO relationship between compressive strength and modulus of elasticity appears to be reasonably consistent with the measured data for strength levels up to 12,000 psi (83 MPa). However, correlation between the AASHTO expression and the measured data appears to diminish somewhat for higher compressive strength levels.

The data shown in Figure 8 indicate that the AASHTO relationship may tend to overestimate the modulus of elasticity for concrete with compressive strength exceeding 12,000 psi (83 MPa). Consequently, it is recommended that LADOTD consider using values that are slightly less than those predicted by the AASHTO expression whenever design concrete compressive strengths exceed 12,000 psi (83 MPa). It is also recommended that the state continue to build upon their existing high-strength concrete modulus of elasticity database for the purpose of determining suitable reduction factors that could be applied to the AASHTO expression when needed.

Modulus of Rupture

Concrete modulus of rupture tests were performed in accordance with ASTM C 78 at an age of 56 days. Concrete modulus of rupture versus compressive strength data for the four instrumented girders is presented in Figure 9. For the purpose of comparison, measured data obtained from other previous HPC research sponsored by LTRC is also shown in Figure 9 *[1]*, *[2]*, *[3]*. The solid lines shown in Figure 9 represent calculated relationships between concrete compressive strength and modulus of rupture using the expression $f_r = k \sqrt{f'_c}$, where the k factor is taken as either 7.5 (lower line) or 10 (upper line). The $f_r = 7.5 \sqrt{f'_c}$ line represents the relationship for modulus of rupture given in Article 9.15.2.3 of the *AASHTO Standard Specifications for Highway Bridges,* where the f'_c and f_r terms are used in psi units, or the expression $f_r = 0.24 \sqrt{f'_c}$ given in Article 5.4.2.6 of the *AASHTO LRFD Bridge Design Specifications* where the f'_c and f_r terms are used in ksi units *[5]*, *[7]*.

In the *AASHTO LRFD Bridge Design Specifications*, the expression $f_r = 0.24 \sqrt{f'_c}$ is used to calculate cracking moment term needed to evaluate crack control by distribution of reinforcement (Article 5.7.3.4) and deflection/camber deformations (Article 5.7.3.6.2). The *AASHTO LRFD Bridge Design Specifications* also allows for a higher f_r value ($f_r = 0.37 \sqrt{f'_c}$) when calculating the cracking moment used to evaluate minimum reinforcement provisions (Article 5.7.3.3.2). The upper line shown in Figure 9 represents the expression $f_r = 0.37 \sqrt{f'_c}$.

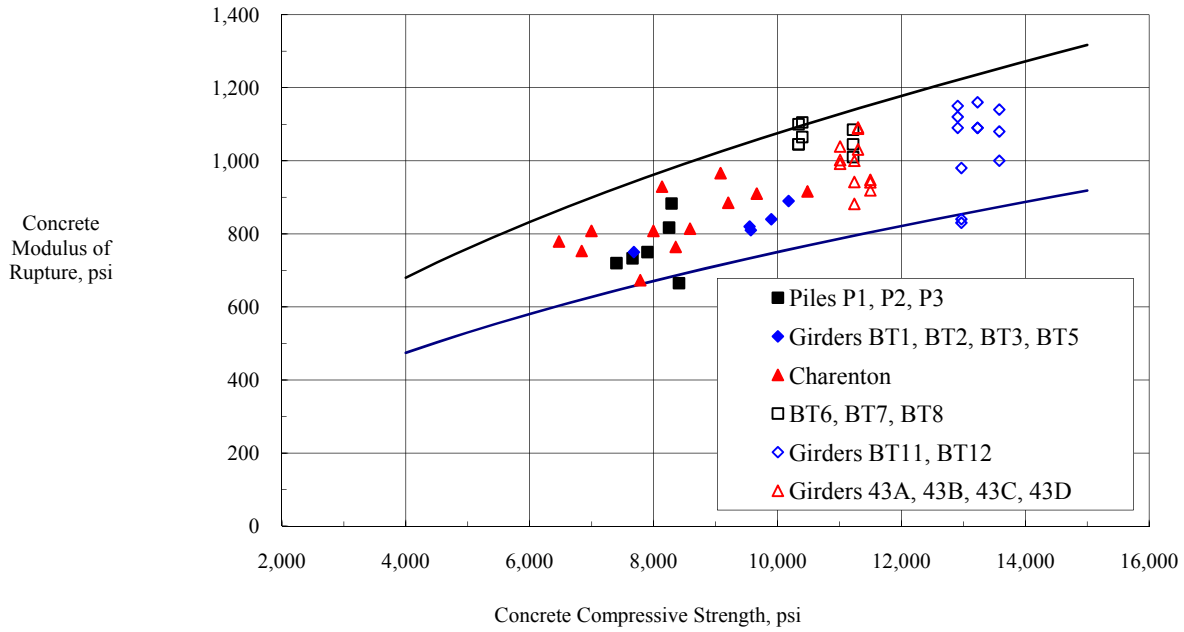

Figure 9
Concrete modulus of rupture versus compressive strength

As indicated by the data presented in Figure 9, the *AASHTO Standard Specifications for Highway Bridges* and *LRFD Bridge Design Specifications* equations corresponding to the lower solid line appear to consistently provide a conservative prediction of modulus of rupture for all strength levels investigated. The variability of the measured modulus of rupture data is such that the use of the higher $f_r = 0.37\sqrt{f'_c}$ value currently incorporated in the *AASHTO LRFD Bridge Design Specifications* for anything other than evaluating minimum reinforcement requirements does not appear warranted.

Chloride Permeability

Tests to determine the chloride permeability of the girder concrete were performed in accordance with ASTM C 1202 on field-cured 6 x 12-in. (152 x 305-mm) cylinders representing concrete place in the midspan of each instrumented girder. The chloride permeability tests were performed at a concrete age of 56 days. The average chloride permeability determined for the concrete used in the midspan region of Girders 43A, 43B, 43C, and 43D was 151 coulombs. This average measured permeability value is considerably less than the 2,000 coulomb limit stipulated in the specifications for the Rigolets Pass Bridge project.

The average measured permeability value for the Rigolets Pass Bridge project is also considerably less than the average permeability value for the Charenton Canal Bridge project (1,355 coulombs) measured at a concrete age of 56 days *[2]*. The concrete mix design for the girders in the Charenton Canal Bridge incorporated 30 percent Class C fly ash by total weight of cementitious materials. The HPC girders in the Rigolets Pass Bridge incorporated 11 percent silica fume by total weight of cementitious materials. Therefore, the use of silica fume provides a much greater benefit relative to decreasing overall permeability than Class C fly ash.

Coefficient of Thermal Expansion

Tests to determine the coefficient of thermal expansion for the girder concrete were performed in accordance with CRD-C39 on field-cured 6 x 12-in. (152 x 305-mm) cylinders representing concrete placed in the midspan of Girder 43D. It was originally planned that coefficient of thermal expansion tests would be performed at concrete ages of 3 and 90 days. However, due to problems encountered during testing, the data for the 3-day test age was judged unreliable and was subsequently discarded and replaced with data from another test performed at an age of 28 days. The average coefficient of thermal expansion for the girder concrete measured at test ages of 28 and 90 days were 4.45 millionths/ºF (8.01 millionths/ºC) and 5.54 millionths/ºF (9.97 millionths/ºC), respectively. The overall average coefficient of thermal expansion for both test ages was 5.00 millionths/ºF (9.00 millionths/ºC). This average measured value was subsequently used to correct measured concrete strains for temperature effects prior to use in prestress loss calculations.

Creep and Shrinkage

Tests to determine creep and shrinkage properties for the girder concrete were performed in accordance with ASTM C512 on field-cured 6 x 12-in. (152 x 305-mm) cylinders representing concrete placed in the midspan region of Girder 43D. It was originally planned that creep and shrinkage tests would be started at concrete ages of 3 and 90 days. However, due to delay in receiving the cylinders for the 90-day test age, the actual concrete age at the time the test commenced was 100 days. Both the 3- and 100-day age creep and shrinkage tests were performed under ambient conditions of 73ºF (23ºC) and 50 percent relative humidity. The planned test duration used for each age of loading was one year. However, the duration of the 3-day age of loading test was extended to terminate at the same time as the 100-day age of loading test.

Prior to starting the creep tests, additional representative field-cured 6 x 12-in. (152 x 305-mm) cylinders were tested in compression to determine compressive strength corresponding with each age of loading. Three cylinders were tested for each age. The measured concrete compressive strength for concrete ages of 3 and 90 days were 8,250 psi (57 MPa) and 12,210 psi (84 MPa), respectively. These average compressive strength values were used as the basis for establishing the intensity of the load used for the creep tests. For both test ages, the target applied load used for creep testing corresponded to 40 percent of the measured concrete compressive strength at that age; 3300 psi (23 MPa) for 3-day tests and 4,880 psi (34 MPa) for the 100-day tests

Measured creep coefficient, defined as the ratio of creep strain to initial strain, and shrinkage data for the two different ages of loading (3 and 100 days) are shown in Figures 10 and 11, respectively. The initial strain used to calculate creep coefficient was taken as the average measured deformation resulting from the initial application of load. Also included in Figures 10 and 11 are corresponding calculated values for the 3-day age of loading determined using provisions from the *AASHTO LRFD Bridge Design Specifications [7]*. According to Article 5.4.2.3 of the *AASHTO LRFD Bridge Design Specifications*, when mix-specific data are not available, estimates of creep and shrinkage may be made using the provisions of Articles 5.4.2.3.2 and 5.4.2.3.3, respectively. Article 5.4.2.3.2 includes an equation for calculating creep coefficient for various ages after initial loading. Article 5.4.2.3.3 includes an equation for calculating shrinkage at various concrete ages.

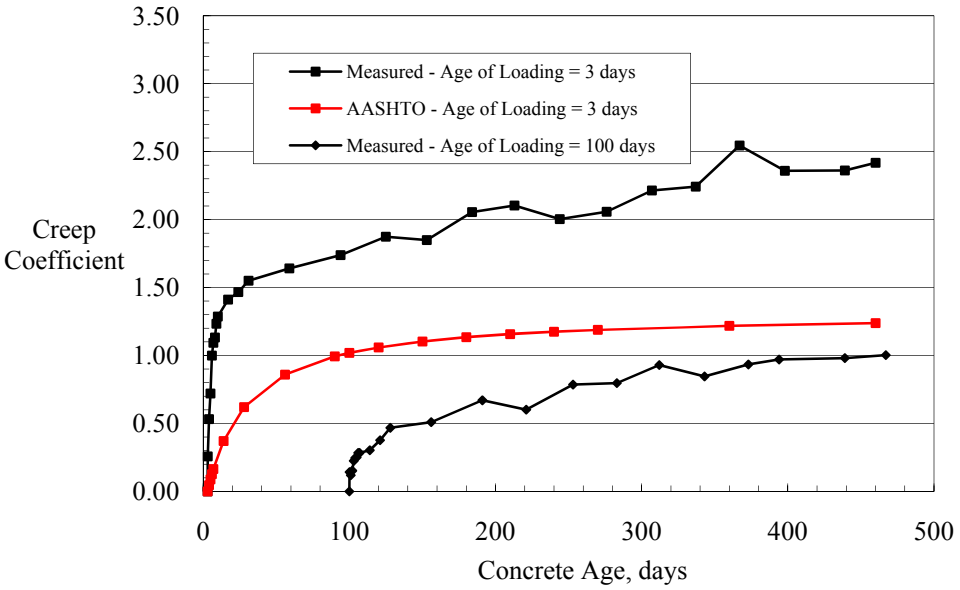

Figure 10
Creep coefficient versus concrete age

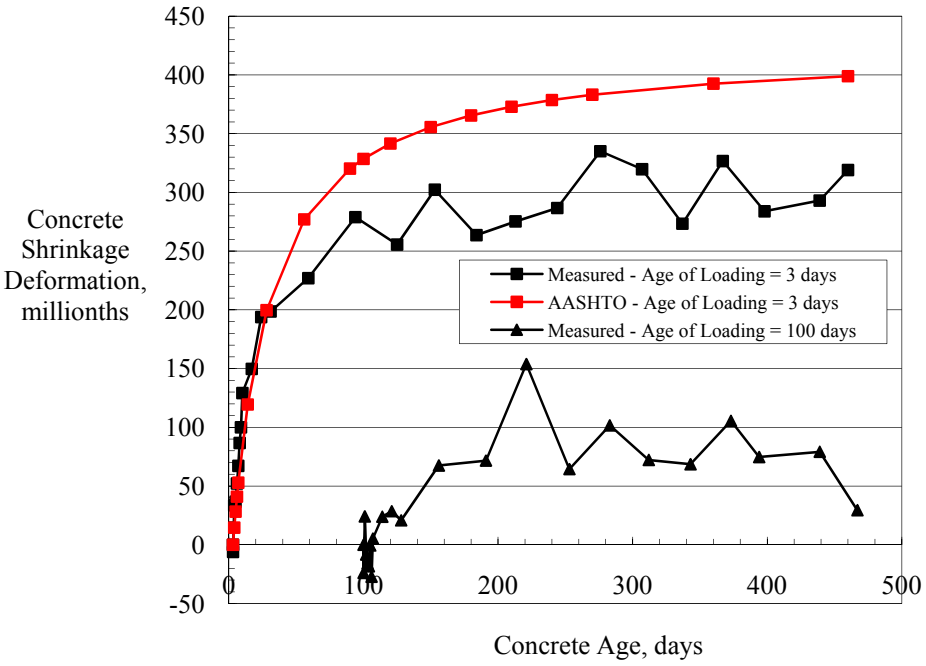

Figure 11
Concrete shrinkage versus age

The measured creep coefficient and shrinkage data shown in Figures 10 and 11 reflect two phenomena typically observed with conventional strength concretes; the rate of creep and shrinkage decreases with time, and the creep coefficient and total shrinkage are less for concrete tests beginning at later ages. Recognizing that the four HPC girders fabricated for the instrumented bridge span first experience compressive stresses and significant drying conditions beginning at the time of form removal and strand release, the creep and shrinkage data for the 3-day age of loading condition would be expected to more closely represent the actual in-service response.

Based on the 3-day age of loading data, the creep coefficient after 12 months stabilized at a value of approximately 2.50, and the shrinkage stabilized at approximately 300 millionths. According to the ACI Committee 209 Report (ACI 209R-92), the ultimate creep coefficient of concrete normally falls in the range of 1.30 to 4.15, and ultimate shrinkage will normally fall into the range of 415 to 1070 millionths *[8]*. The creep coefficient after one year reflected by the measured test data falls approximately in the middle of the expected range. The measured shrinkage after one year falls well below the expected range. Based on these

data, lower-than-normal measured girder prestress losses due to the combined effects of creep and shrinkage would be expected.

Based on the data shown in Figures 10 and 11, it is apparent that the *AASHTO LRFD Bridge Design Specifications* provisions for estimating creep and shrinkage when mix-specific data are not available did not correlate well with the measured data. The final measured creep coefficient value for the 3-day age of loading was approximately twice as great as the corresponding calculated AASHTO estimated value. The final measured shrinkage value for the 3-day age of loading was approximately 75 percent of the corresponding calculated AASHTO estimated value. Consequently, for the HPC placed in the midspan region of Girder 43D, the provisions of Articles 5.4.2.3.2 and 5.4.2.3.3 of the *AASHTO LRFD Bridge Design Specifications* underestimated creep coefficient and overestimated shrinkage.

Prestressing Strand Material Properties

During fabrication of the four instrumented girders for Span 43, samples of 0.6-in. (15.2-mm) diameter prestressing strands were taken and tested to determine breaking strength, 1 percent elongation load (yield), modulus of elasticity, and total elongation. Results from the strand tests are presented in Table 6. All applicable measured strand material properties reported in Table 6 satisfied the corresponding specification requirements of ASTM Designation: A416. As indicated in Table 6, the average measured modulus of elasticity for the seven strand lots tested was 27,950 ksi (193 GPa).

Table 6
Prestressing strand material properties

Strand Lot / Serial Number	1 Percent Elongation Load, lbf	Breaking Load, lbf	Total Elongation Under Load, percent	Modulus of Elasticity, ksi
130146679326	55,200	59,600	6.1	28,300
130146679327	54,900	59,800	6.5	27,050
130146679328	55,200	59,400	5.0	27,850
130146679331	54,800	59,800	5.9	28,250
130146679332	56,000	60,000	5.1	28,650
130146679335	54,800	59,800	5.9	27,700
130146679342	54,800	59,600	6.0	27,950
Average	55,100	59,700	5.8	27,950

Deck Slab Concrete Material Properties

Measurements of compressive strength, modulus of elasticity, modulus of rupture, rapid chloride permeability, and coefficient of thermal expansion were made on test specimens representing concrete placed in the midspan region of the deck slab for Span 43. Measured concrete properties are presented in Table 7.

Table 7
Deck slab concrete material properties

Material Property	Specimen Size	Initial Curing	Cyl.	Concrete Age				
				3 days	7 days	28 days	56 days	90 days
Compressive Strength,[a] psi	6 x 12-in. cyl.	Field	1	—	5,850	7,880	—	8,570
			2	—	5,580	7,790	—	8,870
			3	—	5,600	7,600	—	8,670
			Ave	—	5,677	7,757	—	8,703
Modulus of Elasticity,[a] ksi	6 x 12-in. cyl.	Field	1	—	5,100	5,850	—	6,450
			2	—	5,250	5,350	—	6,350
			3	—	5,050	5,700	—	6,500
			Ave	—	5,133	5,633	—	6,433
Unit Weight,[a] lb./ft^3	6 x 12-in. cyl.	Field	1	—	143.7	145.1	—	145.1
			2	—	144.3	144.2	—	143.9
			3	—	144.6	144.7	—	144.7
			Ave	—	144.2	144.7	—	144.6
Modulus of Rupture,[a] psi	6 x 6 x 20-in. beam	Field	1	—	—	730	630	—
			2	—	—	760	640	—
			3	—	—	800	590	—
			Ave	—	—	763	620	—
Permeability,[a] Coulombs	6 x 12-in. cyl.	Field	1	—	—	—	1,115	—
			2	—	—	—	1,146	—
			3	—	—	—	824	—
			Ave	—	—	—	1,028	—
Coefficient of Thermal Expansion,[a] millionths/ºF	6 x 12-in. cyl.	Field	1	6.47	—	—	—	5.93
			2	5.58	—	—	—	5.40
			3	6.11	—	—	—	5.35
			Ave	6.05	—	—	—	5.56
			Overall Average = 5.81					

a Each reported test value represents one individual tests. Average values represent results from three individual tests.

— Test not performed at designated age.

The specified concrete compressive strength for the deck slab is 4,200 psi (29 MPa) at 28 days. As indicated by the data reported in Table 7, the measured concrete compressive strengths at all test ages exceeded the specified strength.

Tests to determine the chloride permeability of the deck slab concrete were performed in accordance with ASTM C1202 on field-cured 4 x 8-in. (102 x 203-mm) cylinders representing concrete place at midspan. The chloride permeability tests were performed at a concrete age of 56 days. As indicated by the data reported in Table 7, the average measured chloride permeability for the deck slab concrete was 1,028 coulombs. This average measured permeability value is less than the 2,000-coulomb limit stipulated in the specifications for the Rigolets Pass Bridge project.

Prestressing Forces

Each girder was fabricated using uncoated, Grade 270 (1860 MPa), low-relaxation, seven-wire strand conforming to ASTM A416. The specified initial tensile force for each 0.6-in. (15.2-mm) diameter strand was 43.95 kips (195.9 kN), which corresponds to 75 percent of the specified minimum strand breaking strength. During fabrication of the four instrumented girders for Span 43, load cells were installed on six selected prestressing strands between the dead end anchorage and the bulkhead. Strands selected for load cell instrumentation are shown in Figure 4. Using these load cells, the force levels in the selected strands were measured at various time- or event-based intervals, beginning at the time of initial tensioning and continuing until release.

The four instrumented girders were fabricated during two separate production runs. The first production run included instrumented girders 43A and 43B. The second production run included girders 43C and 43D. Average measured strand force values for both production runs recorded after stressing all strands and just prior to release are shown in Table 8. Each value reported in Table 8 represents the average reading for five of the six load cells. During stressing, one of the six load cells tipped due to inadequate bearing support on the bulkhead surface. Upon discovering this condition, the load cell was removed and the strand was re-stressed without load cell instrumentation. This incident occurred for both production runs.

As indicated by the data in Table 8, the average measured force levels after stressing all of the strands were 4.4 to 4.9 percent less than the specified 43.95 kip (195.5 kN) initial force. However, these measured reduction values were still within the 5 percent tolerance cited in the Precast/Prestressed Concrete Institute (PCI) Manual for Quality Control *[9]*.

Table 8
Measured average strand forces

Girder Production Run	Average measured force after stressing all strands			Average measured force prior to release of prestress		
	kips	kN	Percent reduction	kips	kN	Percent reduction
43A and 43B	42.01	186.9	4.4	40.94	182.1	6.8
43C and 43D	41.80	186.0	4.9	40.04	178.1	8.9
Average	41.90	186.4	4.7	40.49	180.1	7.9
Specified	43.95	195.5	< 5.0	—	—	—

Prior to releasing the prestress, the average force levels were 6.8 to 8.9 percent less than the specified initial force. As indicated in Figure 3, measured concrete temperatures at the time of release were still quite high. Therefore, thermal expansion of the embedded strands likely contributed to the reduction in prestress force reported in Table 8. It should also be noted that the overall time duration between stressing and release for the production run incorporating Girders 43C and 43D (70.5 hours) was longer than the duration for the production run incorporating Girders 43A and 43B (48 hours). This difference in overall production duration may have contributed to the noted difference in the measured force reduction between the two production runs.

Prestress Losses

Vibrating wire strain gages (VWSGs) were installed at midspan in each of the four instrumented HPC girders of Span 43, as shown in Figure 5. For each of these girders, the three VWSGs installed in the bottom flange at the center of gravity of the prestressing strands were used to determine prestress losses. The two VWSGs installed in the top flange of each girder provided a second reference point for girder section strain measurements, which could be used as a means of validating the overall response to creep, shrinkage, and temperature deformations as well as external load effects. Each VWSG included a thermistor for measuring concrete temperature associated with each strain measurement. Plots of average measured concrete strain versus time for VWSGs installed in the top and bottom flange of each girder are shown in Figure 12.

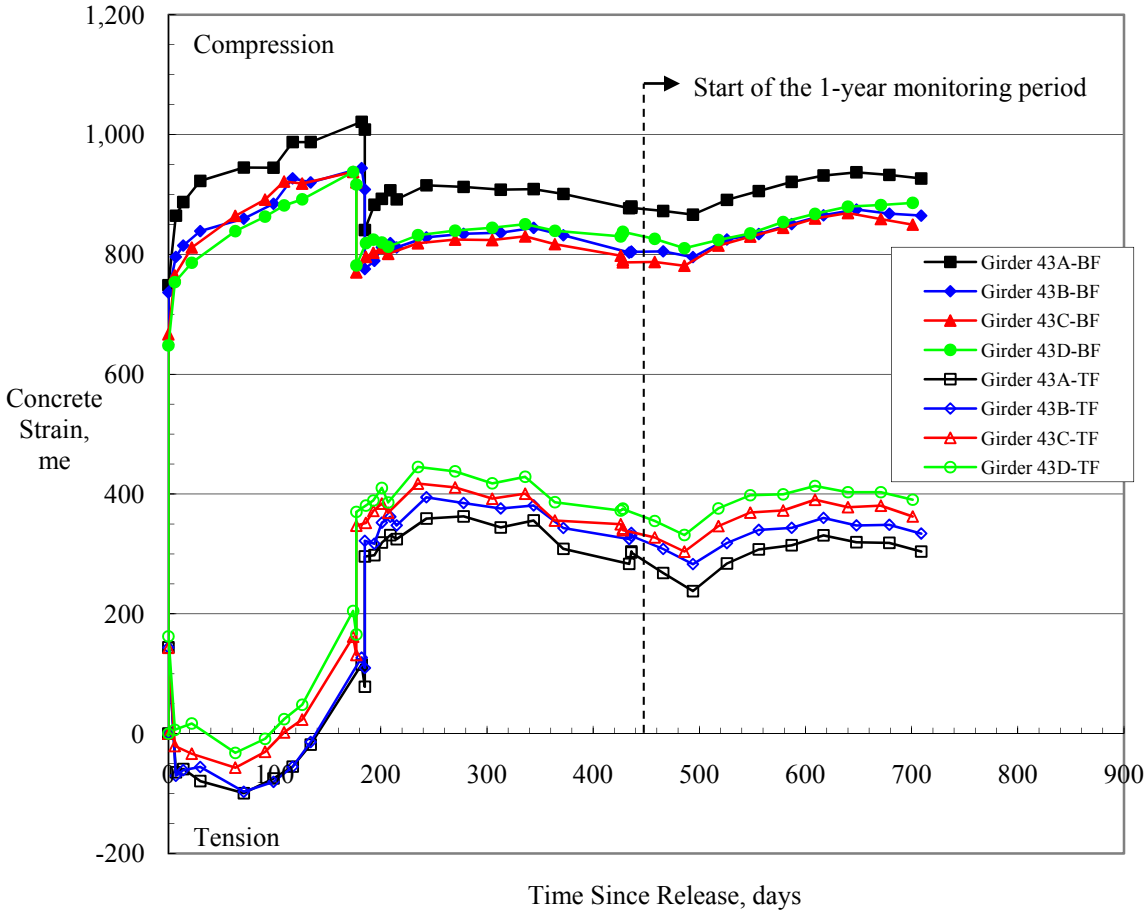

Figure 12
Measured concrete strain versus time for Girders 43A, 43B, 43C, and 43D

The plotted average values shown in Figure 12 were based on individual strain readings that were adjusted to a constant temperature. The temperature correction applied to the individual strain readings was calculated based on the measured concrete temperature associated with the reading, the average measured coefficient of thermal expansion of the girder concrete, and the coefficient of thermal expansion of the strain gage wire provided by the manufacturer. Therefore, the plotted average values in Figure 12 represent corrected strains that theoretically do not include effects due to temperature change.

Strain readings taken just prior to release of the strands served as the zero reference for the average concrete strains reported in Figure 12. After strand release, the average compressive strains measured in the bottom flange gradually increased due to the effects of creep and shrinkage until the time when the deck slab was added. The corresponding measured strains in the top flange essentially mirrored the behavior of the bottom flange until about 80 days, when the readings exhibited maximum tension).

During the time period bounded by the dates of erection (between 126 and 134 days after strand release) and deck casting, the compressive strain in the bottom flange continued to increase while the top flange strains transitioned from slight tension to compression. The gradual load additions resulting from the diaphragms, formwork, and deck slab reinforcing steel did not produce noticeable changes in the bottom flange strains. However, the effects of these additions were evident in the measured top flange strains. The average data plotted in Figure 12 indicate a marked reduction in the bottom flange compressive strain and corresponding increase in the top flange compressive strain occurring 185 days after release, denoting the elastic response due to placement of the deck slab concrete.

The measured concrete strain changes at the center of gravity of the prestressing strands were used to quantify prestress loss parameters caused by elastic shortening, concrete creep, and concrete shrinkage. Using the compatibility assumption that the changes in concrete strain measured at the center of gravity of the prestressing strands are equal to the corresponding average steel strain changes, the measured values reported in Figure 12 can be used to calculate prestress losses using the modulus of elasticity of the strand.

When the bottom flange strain data shown in Figure 12 are edited to remove elastic strain effects resulting from external loading and multiplied by the average measured modulus of elasticity of the prestressing strand equal to 27,950 ksi (193 GPa) reported in Table 6, the resulting plot of prestress loss shown in Figure 13 results. The data plotted in Figure 13 represent the total measured prestress loss in each girder due to the combined effects of elastic shortening, concrete creep, and concrete shrinkage for a time interval beginning at release of the prestressing strands and ending at the conclusion of the one-year monitoring period.

For comparison with the measured data, prestress losses were calculated for a typical interior girder using the provisions of the *AASHTO Standard Specifications for Highway Bridges [5]*. Prestress loss calculations were made to evaluate two different scenarios. The first scenario represents the "design" condition where the calculated loss parameters are based on specified material properties and the assumption that the initial strand stress equals 75 percent of the 270 ksi (1862 MPa) ultimate stress. The second scenario represents the "constructed" condition, where the calculated loss parameters are based on measured material properties and the average strand stress at time of release determined from load cell readings performed during girder fabrication. Specific conditions associated with the two prestress loss calculation scenarios are given in Table 9.

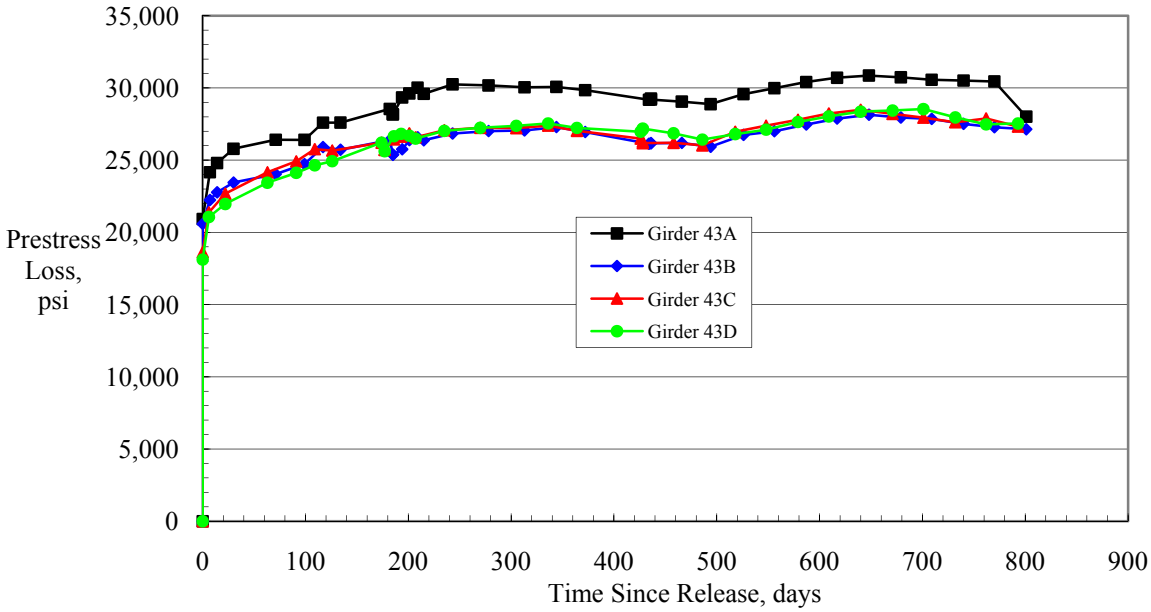

Figure 13
Average prestress loss versus time

Table 9
Prestress loss calculation scenarios

Calculation Parameter	Calculation Scenario	
	Design	Constructed
Girder concrete f'_{ci}, psi	6,670	9,250
Girder concrete E_{ci}, ksi	4,951[a]	6,000
Girder concrete f'_c, psi	10,000	11,260 (56 days)
Girder concrete E_c, ksi	6,062[a]	6,300 (56 days)
Girder unit weight, pcf	155	153 (56 days)[b]
Deck slab f'_c, psi	4,200	7,760 (28 days)
Deck slab Ec, ksi	3,929[a]	5,650 (28 days)
Deck slab unit weight, pcf	150	153 (28 days)[c]
Haunch thickness, in.	2	2
Effective prestress, psi	186,300	171,495
Strand modulus of elasticity, ksi	28,000	27,950

a *Calculated based on an assumed concrete unit weight of 150 pcf and* $E_c = w_c^{1.5}\, 33\sqrt{f'_c}$.

b *Based on average measure concrete unit weight at 56 days equal to 146 pcf plus an estimated additional 7 pcf to account for the weight of the prestressing strand and reinforcement.*

c *Based on average measure concrete unit weight at 28 days equal to 145 pcf plus an estimated additional 8 pcf to account for the weight of the deck slab reinforcement.*

For the "design" scenario, the effective prestress used to determine f_{cir} was taken as 92 percent of the initial stress (as allowed by Article 9.16.2.1.2 of the *AASHTO Standard Specifications for Highway Bridges* for low-relaxation strand), which equals 186,300 psi (1,285 MPa). For the "constructed" scenario, the effective prestress was determined using an iterative approach, where tendon stress values used to calculated f_{cir} were assumed and revised until the resulting elastic shortening loss reduction equaled the assumed prestress loss value. The result was an effective prestress equal to 171,495 psi (1,183 MPa), which corresponds to a reduction of approximately 8.1 percent from the initial stress measured by the strand load cells.

Measured and calculated prestress losses for the interior HPC girders of Span 43 are given in Table 10. The tabulated prestress losses are presented in terms of the four loss components defined in the *AASHTO Standard Specifications for Highway Bridges*; namely, elastic shortening, shrinkage, creep, and relaxation *[5]*. Measured elastic shortening prestress loss was determined based on the average initial concrete strain change resulting from release of the prestress force. Subsequent increases in the measured concrete compressive strain, exclusive of reductions caused by external load effects, were used to quantify prestress loss due to the combined effects of girder concrete shrinkage and creep. The measured shrinkage and creep loss components are lumped together in Table 10 because it is not possible to distinguish the individual contribution from each effect based on the measured strain change alone. The measured prestress loss due to steel relaxation cannot be discerned from the measured strain data and, therefore, is not included among the measured losses. However, the relaxation loss component is generally small in comparison with other loss components, making up only approximately 1 to 2 percent of the total prestress loss.

Table 10
Measured and calculated prestress losses using AASHTO Standard Specifications

Prestress Loss Component	Measured Losses, psi	Calculated Losses, psi	
		Design	Constructed
Elastic Shortening	19,560	20,350	15,100
Shrinkage	8,710[a]	5,750	5,750
Creep		33,920	29,450
Relaxation	—	980	1,730
Total	28,270	61,000	52,030

a Based on maximum total prestress loss measured approximately 650 days after strand release.

As indicated by the data in Table 10, the measured elastic shortening prestress loss correlated well with the corresponding "design" calculated loss. Correlation between the measured elastic shortening loss and corresponding "constructed" calculated loss was not as favorable. The calculated elastic shortening loss is dependent on the concrete modulus of elasticity at the time of strand release. As indicated in Table 9, the "design" elastic shortening loss was calculated using an assumed concrete modulus of elasticity value of 4,950 ksi (34 GPa), while the "constructed" elastic shortening value was calculated using a measured concrete modulus of elasticity value of 6,000 ksi (41 GPa). The modulus of elasticity value used in the "constructed" elastic shortening loss calculation was measured several hours after the time that release actually took place and, therefore, may have been somewhat greater than the actual concrete modulus of elasticity at the time of strand release.

Another possible explanation for the discrepancy between the measured and "constructed" elastic shortening prestress loss could be that the measured concrete strains resulting from release included some creep and shrinkage loss. The time duration between the pre- and post-release strain readings for the four instrumented girders was typically about 1.5 hours. The post-release readings were typically taken within 20 minutes after the conclusion of strand release. While efforts were made to minimize the elapsed time between the pre- and post-release strain measurements, it is likely that the resulting measured change in strain occurring over this time interval included some creep and shrinkage loss.

As shown in Figure 13, the measured prestress loss for each girder gradually increased from the time of strand release until approximately 340 days after release. From that point, the measured losses decreased slightly over the next 160 days and then began to increase again from approximately 500 days until reaching an apparent maximum value approximately 650 days after release. There are two readily-apparent explanations for the observed fluctuation in measured prestress loss. One explanation is that the temperature compensation applied to the measured strains is not precise, causing seasonal temperature variations to have a slight, yet noticeable, effect on the measured prestress loss. The second explanation relates to shrinkage of the deck slab concrete. Deck slab shrinkage will tend to reduce bottom flange compressive strains. Consequently, the measured prestress losses plotted in Figure 13 beyond 185 days include increases due to the combined effect of continuing creep and shrinkage of the girder concrete and reductions due the progression of deck slab shrinkage. Although the measured prestress losses plotted in Figure 13 likely include some negating effects due to deck slab shrinkage, the observed fluctuations appear to be more consistent with the seasonal temperature variation causation scenario than the deck slab shrinkage causation scenario.

The total measured prestress loss value reported in Table 10 is based on the average of the maximum prestress loss values for each interior girder typically occurring approximately 650 days after release. As indicated by the data in Table 10, the total measured prestress loss is approximately 50 percent of the corresponding "design" and "constructed" calculated total prestress loss values. The calculated prestress losses should be viewed as ultimate (end of service life) values. Therefore, total losses measured within the first few years of service would be expected to be less than calculated values. However, according to PCI's "Recommendations for Estimating Prestress Losses," 74 percent of the ultimate creep and 86 percent of the ultimate shrinkage would be expected to have taken place within the first year *[10]*. Applying these percentages to the calculated creep and shrinkage loss values, total prestress losses equal to 51,380 psi (354 MPa) and 43,560 psi (300 MPa) would be expected after one year of service for the "design" and "constructed" scenarios, respectively. The total measured prestress loss is approximately 60 percent of the calculated losses that would be expected after one year. Based on this observation, it is likely that the total final prestress loss measured at the end of service life will be considerably less than the final calculated loss values reported in Table 10.

Based on the data in Table 10, it can be concluded that the prestress losses calculated using provisions outlined in the *AASHTO Standard Specifications for Highway Bridges* may tend to over-estimate actual losses occurring in service. However, the measured losses reported in Table 10 do not include the initial reduction in strand force measured during girder fabrication. As indicated in Table 8, strand load measurements made during girder fabrication indicated an average of 7.9 percent reduction in prestress force occurring prior to release. This measured reduction in strand force translates to a prestress loss of 15,945 psi (110 MPa). As indicated in Figure 3, internal concrete temperatures increased rapidly after placing the concrete and remained quite high at the time of strand release. Based on this observation, it is apparent that a portion of the strand force reduction noted prior to release was likely due to thermal expansion of the strand. In addition, depending upon when bond is established between the strand and concrete, a portion of this measured loss would likely have been recovered upon subsequent cooling of the concrete. Nonetheless, the measured reductions in strand force prior to release greatly exceeded calculated allowances for steel relaxation and thermal expansion and likely constituted an additional source of significant prestress loss not specifically addressed by existing design provisions nor included in the measured losses reported in Table 10.

Measured prestress losses that were considerably less than corresponding design losses calculated using provisions from the *AASHTO Standard Specifications for Highway Bridges* have been reported in previous HPC research sponsored by LTRC *[1]*, *[2]*. Measured long-

term prestress loss in Girder BT3 from the feasibility evaluation research program was approximately 50 percent of the corresponding calculated design value *[1]*. The average measured prestress loss for the instrumented girders in the Charenton Canal Bridge was approximately 67 percent of the corresponding calculated design value *[2]*. The HPC girders in the Rigolets Bridge and Girder BT3 from the feasibility evaluation were made with concrete incorporating approximately 10 percent silica fume by weight of cementitious materials, whereas the Charenton Girders were made using concrete incorporating 30 percent Class C fly ash by weight of cementitious materials. Therefore, there is some evidence to suggest that the use of silica fume may provide a greater benefit to reducing total prestress loss than Class C fly ash.

For further comparison with the measured data, prestress losses were also calculated for a typical interior girder using the latest provisions of the *AASHTO LRFD Bridge Design Specifications, 4th Edition (Including 2008 Interims)* defined in Sections 5.9.5.2.3 and 5.9.5.3 *[7]*. Prestress loss calculations were made using the same two scenarios ("design" and "constructed") as used in the previous calculations (reported in Table 9), with the exception of the effective prestress. The Δf_{pES} for both "design" and "constructed" conditions were calculated using Equation C5.9.5.2.3a-1 of the *AASHTO LRFD Bridge Design Specifications Commentary* to avoid having to initially estimate prestress after transfer and perform multiple iterations with Equation 5.9.5.2.3a-1. In Equation C5.9.5.2.3a-1, the stress in the strand immediately prior to transfer (f_{pbt}) was taken as 202,500 psi (1,396 MPa) for the "design" condition and 186,590 psi (1,287 MPa) for the "constructed" condition. The "design" f_{pbt} value corresponds to 75 percent of the specified minimum strand breaking strength. The "constructed" f_{pbt} value corresponds to the average measured strand force prior to release divided by the nominal strand area. The resulting Δf_{pES} values were subsequently confirmed using Equation 5.9.5.2.3a-1. Measured and calculated prestress losses for the HPC girders of Span 43 are given in Table 11.

As indicated by the data in Table 11, the calculated Δf_{pES} loss for both the "design" and "constructed" conditions were nearly equal to the corresponding calculated elastic shortening loss reported in Table 10. This finding was expected since the equation for Δf_{pES} cited in the *AASHTO LRFD Bridge Design Specifications* (Eq. 5.9.5.2.3a-1) is essentially the same as the equation for the elastic shortening prestress loss cited in the *AASHTO Standard Specifications for Highway Bridges* (Eq. 9-6).

Table 11
Measured and calculated prestress losses using the *AASHTO LRFD Bridge Design Specifications*

Prestress Loss Component	Measured Losses, psi	Calculated Losses, psi	
		Design	Constructed
Δf_{pES}	19,560	19,810	15,100
Δf_{pLT}	8,710[a]	23,620	17,470
Total	28,270	43,430	32,570

a Based on maximum total prestress loss measured approximately 650 days after strand release.

Time-dependent prestress losses (Δf_{pLT}) were calculated using the approximate method defined in Section 5.9.5.3 of the *AASHTO LRFD Bridge Design Specifications [7]*. The calculated Δf_{pLT} loss for both the "design" and "constructed" conditions shown in Table 11 were considerably greater than the average creep and shrinkage loss measured in the interior girders of Span 43 since the time of release. However, these calculated Δf_{pLT} loss values are considerably less than the corresponding calculated combined creep, shrinkage and relaxation values shown in Table 10 for the *AASHTO Standard Specifications for Highway Bridges* method *[5]*.

The total prestress loss predicted using the *AASHTO LRFD Bridge Design Specifications* method provided better correlation with the total measured loss data for the interior girders of Span 43 than the total prestress loss predicted using *AASHTO Standard Specifications for Highway Bridges* method. As indicated by the data in Table 11, the total measured prestress loss is approximately 65 and 87 percent of the corresponding "design" and "constructed" calculated total prestress loss values, respectively.

Girder Deflections

During fabrication, three elevation reference points were embedded along the top flange of each of the four instrumented girders. These points were embedded at midspan and near both ends to provide a permanent reference for girder defection measurements. Prior to casting the deck slab, the elevation reference points embedded in the top surface of each girder were extended to the elevation of the finished surface of the deck slab.

Girder deflection measurements were made using a standard surveyor's level and custom rod with smallest measurement divisions of 1/16 in. (1.6 mm). Deflection measurements

were made using the level to sight elevations at each reference point location. Based on these measurements, the deflection was calculated by subtracting the average elevation of the two girder ends from the midspan elevation.

During construction, girder midspan deflection measurements were made prior to strand release, after strand release, after girder storage, at a concrete age of 28 days, once a month for the next two months, before shipping, after erection, and before and after deck casting. After casting the deck slab, deflection measurements were made once a week for the first month, once a month for the first three months, and every six months during the one-year monitoring period. The measured midspan deflection versus time for each of the four instrumented girders is shown in Figure 14.

The positive deflection values shown in Figure 14 represent a net upward deflection (camber), initiating at the time of prestressing strand release. The plotted deflection data indicate a marked reduction in camber occurring approximately 185 days after release, denoting the elastic response due to placement of the deck slab concrete.

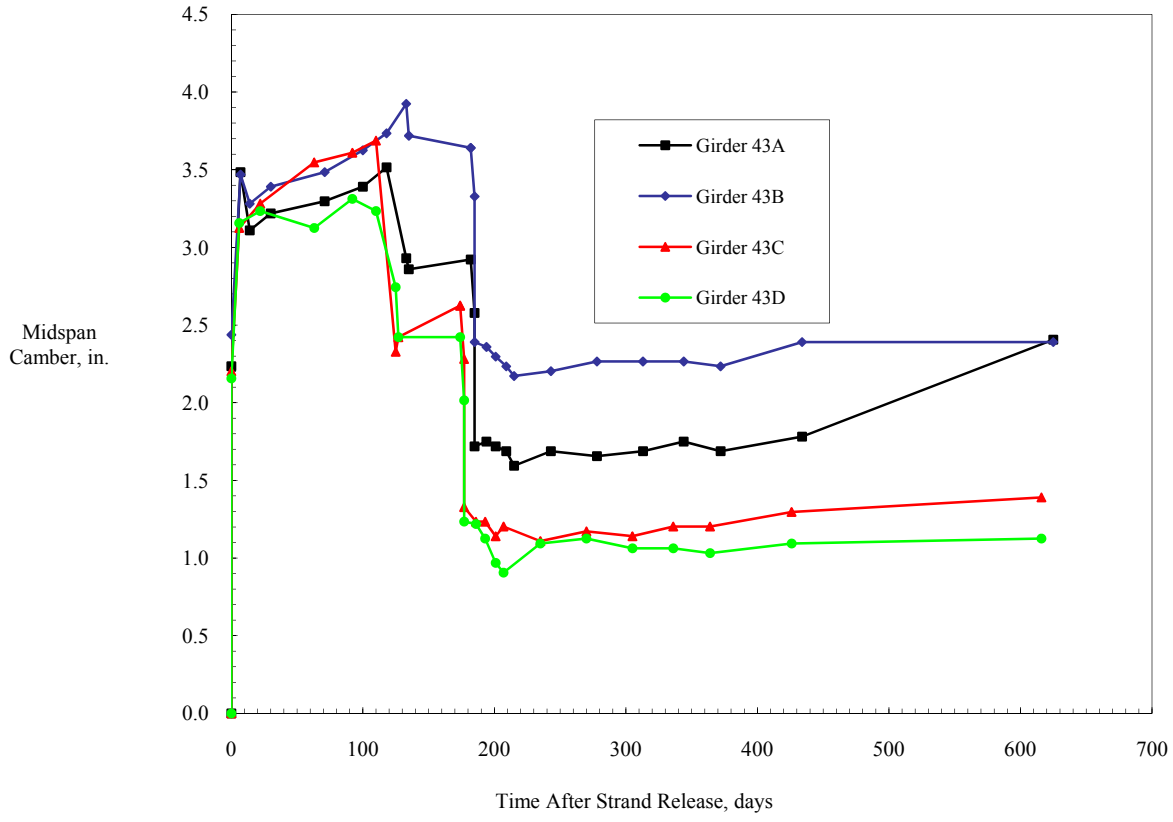

Figure 14
Measured midspan deflection versus time

Average measured deflections and corresponding calculated deflections are given in Table 12 for various stages of construction. The tabulated calculated deflection values are for a typical interior girder, and include both the "design" and "constructed" scenarios previously used for the prestress loss calculations. Deflection calculations were carried out using a traditional moment-area approach along with girder and deck slab properties shown in Table 9.

Table 12
Measured and calculated girder deflections

Time After Release, days	Construction Stage	Measured Deflection, in		Calculated Deflection, in.	
		Range	Average	Design	Constructed
0.01	After release[a]	2.16-2.44	2.26	3.08	2.24
6-7	Girder storage[b]	3.13-3.48	3.31	3.08	2.24
110-118	Before shipment	3.23-3.73	3.54	3.08	2.24
177-185	Before deck cast	2.42-3.64	2.90	3.08	2.24
177-185	After deck cast	1.23-2.39	1.67	1.40	0.59
616-625	Final reading	1.12-2.40	1.83	1.40	0.59

a *Calculated deflection values for the release stage were based on a span equal to the full 130.8-ft end-to-end length of the girder. Calculated values for all other stages were based on the design center-to center distance between bearing supports equal to 129.8 ft.*

b *Calculated deflection values for the storage stage were based on a girder concrete modulus of elasticity equal to the average of the corresponding E_{ci} and E_c values shown in Table 9. All other subsequent calculated values are based on the corresponding E_c values shown in Table 9.*

As indicated by the data in Table 12, the calculated "constructed" deflection values were considerably less than the corresponding calculated "design" deflection values. The difference between these values was partially due to the fact the "constructed" deflections were based on higher (measured) girder concrete modulus of elasticity values than those used for the "design" deflections. The "constructed" deflections were also calculated based on a lower effective prestress force than was used for the "design" deflections, as indicated in Table 9 and described in the associated text. The calculated upward girder deflection resulting from the prestress force alone applied at the time of strand release was 4.77 in. (121 mm) for the "design" condition and 3.62 in. (92 mm) for the "constructed" condition. Therefore, it is apparent that the majority of the difference between the calculated "design" and "constructed" deflection values was due to the difference in prestress force associated with these two scenarios

The initial average measured camber at release was less than the corresponding "design" calculated value, but correlated well with the "constructed" calculated value. Once the girders were moved into storage approximately seven days after release, the average

measured camber was in closer agreement with the "design" calculated value, and was considerably greater than the corresponding "constructed" calculated value. As indicated by the data reported in Table 12, the measured deflections taken after the girders were moved into storage were approximately 50 percent greater than the measured values taken immediately after strand release. The reported increase in measured camber was likely due to concrete temperature effects, the change in support condition resulting from moving the girders off of the casting bed, and camber growth effects caused by concrete creep and shrinkage deformations.

During the time period that that girders were stored in the precast yard (approximately 100 days) the average measured deflection increased slightly, from 3.31 in. (84 mm) to 3.54 in. (90 mm). Prior to casting the deck slab, the average measured deflection was 2.90 in. (74 mm), or 0.64 in. (16 mm) less than the "before shipment" value. The camber decrease indicated by the "before deck cast" measurement was likely the result of dead load from the addition of the formwork and deck slab reinforcing steel.

Based on the data reported in Table 12, the average measured change in camber deflection among the four instrumented girders resulting from addition of the deck slab was 1.23 in. (31 mm). The corresponding calculated change in camber deflection for both the "design" and "constructed" conditions was 1.68 in. (43 mm) and 1.65 in. (42 mm), respectively. The average measured value is less than both of the corresponding calculated deflection values. It is interesting to note that the measured change in bottom flange strain due to the addition of the deck slab shown in Figure 12 was also less than what would be expected based on traditional elastic analysis. One possible explanation for this lack of correlation is the influence of deck slab concrete temperature increase on the "after cast" readings. The "after cast" readings were taken after the deck slab concrete had achieved initial set and had begun to generate heat from hydration. During the time period between the "before cast" and "after cast" readings, the temperature of the girder top flange concrete increased by approximately 10ºF (6ºC) due to hydration of the adjacent deck slab concrete. This temperature increase will tend to cause an increase in compressive strain in the bottom flange and a corresponding decrease in the net measured downward deflection resulting from the addition of the deck slab concrete

As indicated by the data reported in Table 12, with the exception of the "after release" construction stage, the calculated deflections for the "design" scenario were in closer agreement with measured values than the calculated deflections for the "constructed" scenario. However, it should be noted that the calculated deflection values reported in Table 12 do not account for the effects of prestress losses resulting for girder concrete creep and

shrinkage deformations, or the effects of shrinkage of the deck slab concrete. The plot shown in Figure 14 indicates a slight but gradual increase in girder midspan camber with time. This subtle increase likely indicates the net effect of these phenomena, with the girder creep and shrinkage outweighing the effect of deck slab shrinkage by a narrow margin. It should also be noted that the girder deflection measurements were taken under a variety of different temperature and cloud cover conditions. Therefore, some of these measurements could have been influenced by concrete temperature gradients occurring within the cross-section of the girders or bridge span.

Deck Strains

Concrete strains at mid-depth of the deck slab were measured at seven transverse locations at mid-length of Span 43. Four of the seven strain gages (S1, S3, S5, and S7) were located directly above the centerline of Girders 43A, 43B, 43C, and 43D. The remaining three strain gages (S2, S4, and S6) were located midway between girders 43A and 43B, 43B and 43C, and 43C and 43D. The lead wire for the gage situated above Girder 43A (S1) was damaged beyond repair during removal of the deck slab side forms. Consequently, no data from this gage could be obtained. A plot of concrete strain versus time for the remaining six gages is shown in Figure 15.

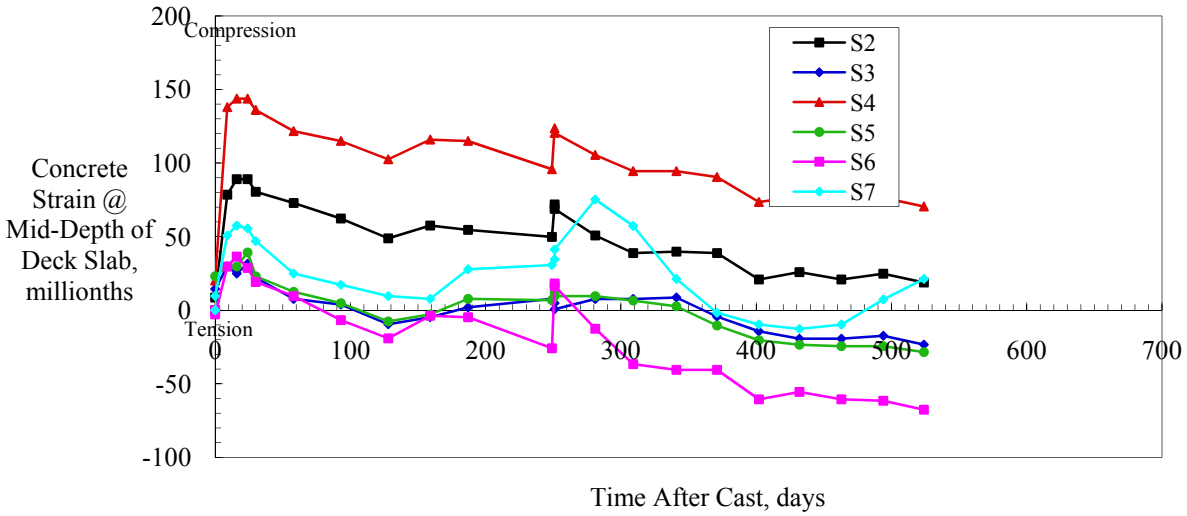

Figure 15
Deck slab concrete strain versus time

As indicated by the data shown in Figure 15, the measured strains from gages installed directly above the girders (S3, S5, and S7) exhibited similar strain levels, while the remaining three gages (S2, S4, and S6) exhibited somewhat variable strain levels. All six gages exhibited a trend of initial compressive strain (presumably due to initial drying shrinkage), followed by a gradual transition to increasing tension. This trend of increasing tension is likely due to the effects of girder creep and shrinkage deformations, and is consistent with the trends seen in the measured girder strains (Figure 12) and the measured girder deflections (Figure 14).

The abrupt increase in deck slab compressive strain occurring at approximately 260 days after concrete placement was likely due to the addition of the barrier railing installed along both sides of the span. As indicated in Figure 15, the effect of the barrier railing addition was more pronounced for gages S2, S4, and S6 (located between girders), than it was for gages S3, S5, and S7 (located above girders).

Seasonal Temperature and Strain Fluctuations

Each of the vibrating wire strain gages installed in the girders and deck slab of Span 43 was connected to an on-site data acquisition system (DAS) with remote access and data collection capabilities. In addition to the vibrating wire strain gages, an external temperature and humidity probe was connected to the DAS for the purpose of monitoring ambient conditions at the bridge site. The DAS was programmed to read and store measured data from each gage once per hour over a one-year monitoring period. The data recorded by the DAS was used to evaluate daily and seasonal fluctuations in both concrete temperatures and strains.

DAS monitoring of Span 43 commenced on January 11, 2008, a few days before the bridge was opened to traffic. Seasonal fluctuations in concrete temperatures and strains were evaluated by examining and comparing the measured hourly data for consecutive days of a typical winter or summer month to represent a range of different weather conditions.

Winter Temperature and Strain Data

Typical winter season fluctuations in measured concrete temperatures and strains were evaluated by examining data recorded during the month of February 2008. Plots of measured temperature data for the entire month of February and for a single selected sunny day during the month are shown in Figure 16.

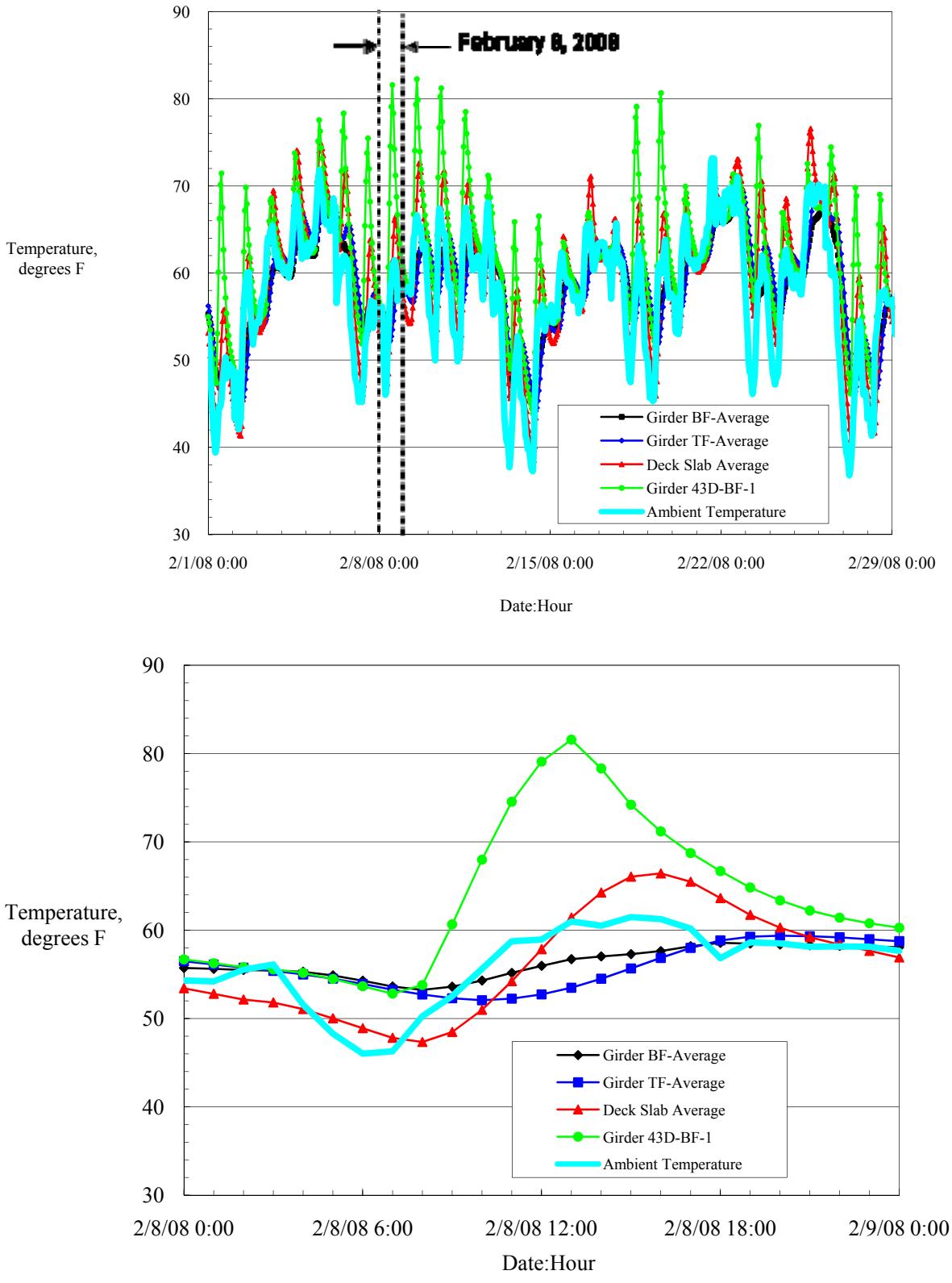

Figure 16
Measured concrete temperature data – February 2008

As expected, average internal concrete temperatures measured in both the girders and deck slab generally followed the corresponding trend of the outside ambient temperature. As indicated by the black and blue plot lines shown in Figure 16, the average internal girder temperatures tended to lag behind the ambient temperature (thick, light-blue line) whenever substantial increases or decreases occurred over a short time period. The average daily high deck slab temperatures tended to slightly exceed the corresponding ambient temperatures on days with minimal cloud cover during afternoon hours, as indicated by the red plot line in Figure 16.

The temperature-sensing element of the vibrating wire strain gage located in the bottom flange of exterior Girder 43D (gage 43D-BF-1) also registered concrete temperatures that exceeded the corresponding ambient temperature as indicated by the green plot line in Figure 16. As shown in Figure 2, exterior Girder 43D is located along the south side of the bridge span. During the winter months, the sun is at a greater angle relative to the south side surface of Girder 43D than to the horizontal surface of the deck slab. Consequently, the south side of Girder 43D receives more solar radiation than the deck slab during a typical sunny winter day and will tend to register higher concrete temperature readings. As indicated in Figure 16, the internal concrete temperature near the south side surface of Girder 43D was as much as 20º F (11º C) greater than the corresponding ambient temperature on some days.

Plots of measured strain data for the entire month of February are shown in Figure17. Unlike the values plotted in Figure 12, the strains shown in Figure 17 have not been corrected to a common temperature. Therefore, the plotted strain values include the effect of temperature variation. Average internal concrete strains measured in both the girders and deck slab generally exhibited daily fluctuations due to changes in ambient conditions. As indicated by the black and red plot lines shown in Figure 17, the average daily concrete strain changes in the bottom flange and deck slab were relatively small, ranging from approximately 0 to 50 millionths. The average daily concrete strain change in the top flange (depicted by the blue plot line in Figure 17) was typically larger and more consistent than that noted in the bottom flange and deck slab, ranging from approximately 50 to 100 millionths.

The vibrating wire strain gage located in the bottom flange of exterior Girder 43D along the south side of the bridge span (gage 43D-BF-1) also registered daily concrete strain fluctuations of as much as 100 millionths as indicated by the green plot line in Figure 17. These strain fluctuations appear to follow the same trend as the concrete temperature fluctuations shown in Figure 16 and were likely accentuated by the effect of increased solar radiation on the southern bridge exposure throughout the year.

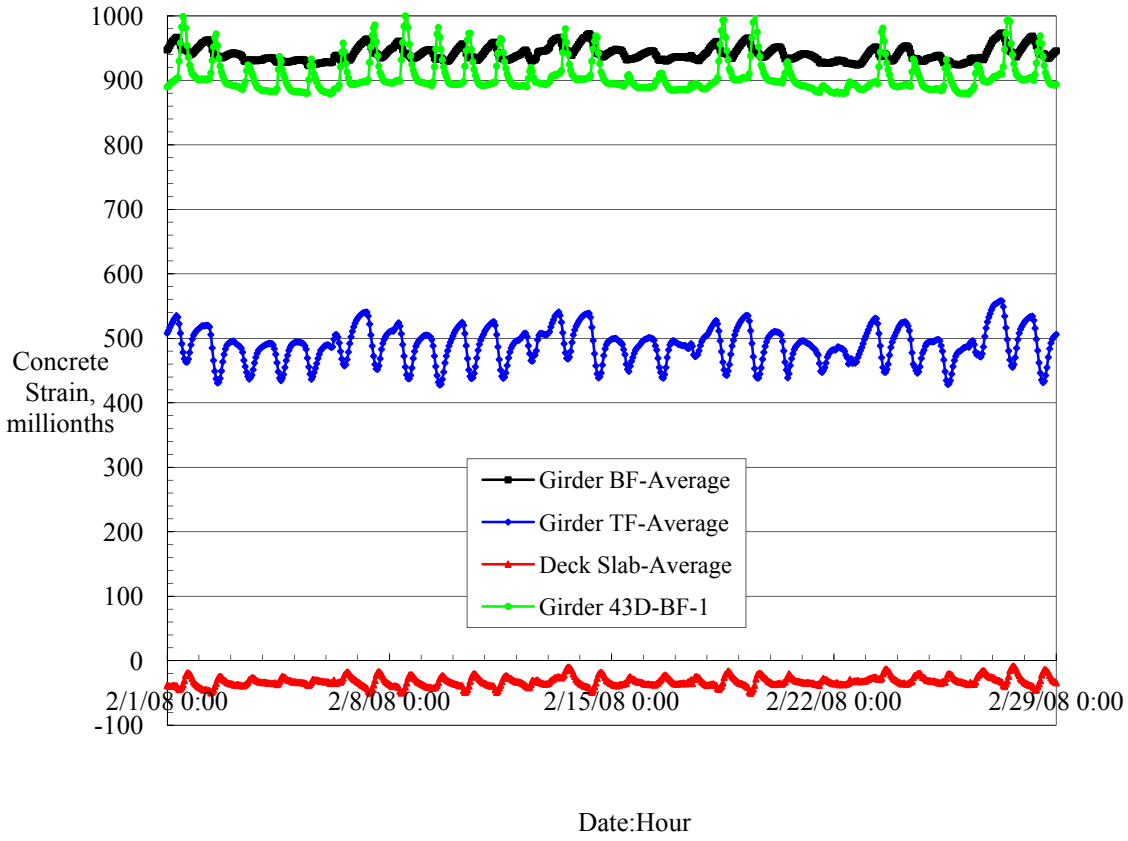

Figure 17
Measured concrete strain data – February 2008

The daily strain fluctuations shown in Figure 17 for the month of February are driven by changes in weather conditions at the bridge site (temperature, cloud cover, precipitation, relative humidity, etc.). Although not sustained for prolonged periods of time, these fluctuations will still have a temporary superimposed effect on both girder and deck slab concrete stress levels. However, quantifying these weather-induced changes in stress levels is a very complex problem, requiring consideration of several parameters including non-linear temperature gradients, material properties, longitudinal continuity of the bridge span, and sources of restraint.

Summer Temperature and Strain Data

Typical summer season fluctuations in measured concrete temperatures and strains were evaluated by examining data recorded during the month of August 2008. Plots of measured temperature data for the entire month of August, and for a single selected sunny day during the month, are shown in Figure 18.

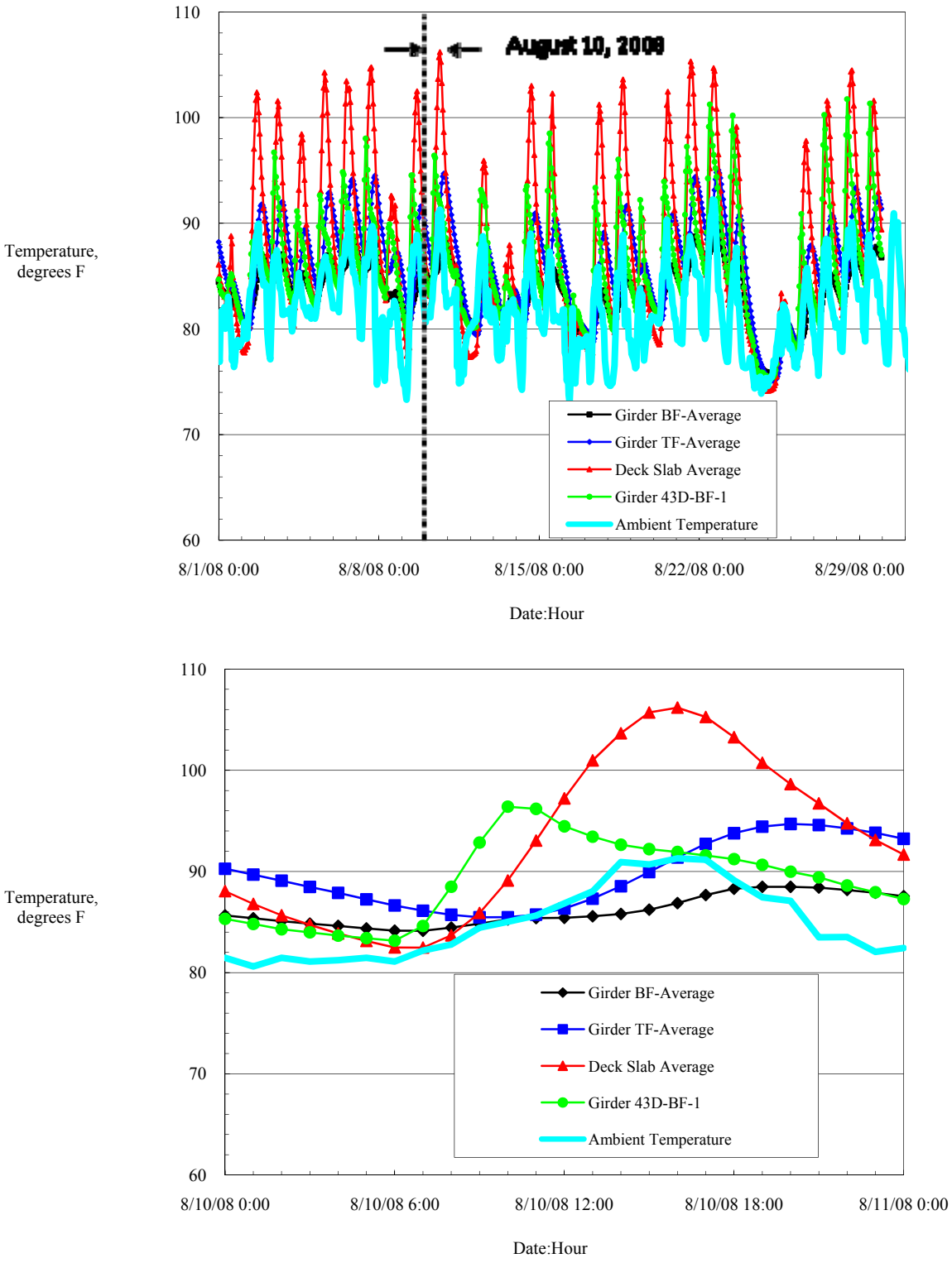

Figure 18
Measured concrete temperature data – August 2008

As previously noted for the winter data, average internal concrete temperatures measured in both the girders and deck slab generally followed the corresponding trend of the outside ambient temperature. However, as indicated by the black plot line shown in Figure 18, the average girder bottom flange internal concrete temperatures tended to lag behind the ambient temperature (thick, light-blue line) whenever substantial increases or decreases occurred over a short time period. The average daily high deck slab and girder top flange temperatures tended to exceed the corresponding ambient temperatures on days with minimal cloud cover during afternoon hours, as indicated by the red and blue plot lines in Figure 18.

The temperature-sensing element of the vibrating wire strain gage located in the bottom flange of exterior Girder 43D (gage 43D-BF-1) also registered concrete temperatures that exceeded the corresponding ambient temperature, as indicated by the green plot line in Figure 18. As shown in Figure 2, exterior Girder 43D is located along the south side of the bridge span. During the summer months, the sun is at a greater angle relative to the horizontal surface of the deck slab than to the south side surface of Girder 43D. Consequently, the deck slab receives more solar radiation than the south side of Girder 43D during a typical sunny summer day and will tend to registered higher concrete temperature readings. As indicated in Figure 18, the average deck slab temperature was as much as 15º F (8º C) greater than the corresponding ambient temperature on some days.

Plots of measured strain data for the entire month of August are shown in Figure 19. Unlike the values plotted in Figure 12, the strains shown in Figure 19 have not been corrected to a common temperature. Therefore, the plotted strain values include the effect of temperature variation. Average internal concrete strains measured in both the girders and deck slab generally exhibited daily fluctuations due to changes in ambient conditions. As indicated by the black and red plot lines shown in Figure 19, the average daily concrete strain changes in the bottom flange and deck slab were relatively small, ranging from approximately 0 to 15 millionths. The average daily concrete strain change in the top flange (depicted by the blue plot line in Figure 19) was typically larger than that noted in the bottom flange and deck slab, ranging from approximately 50 to 100 millionths. The recorded average strain data shown in Figure 19 for typical summer exposure conditions were similar to those shown in Figure 16 for typical winter exposure conditions. However, average daily measured strain fluctuations in the girder bottom flange and deck slab were noticeably more pronounced for winter exposure than for summer exposure.

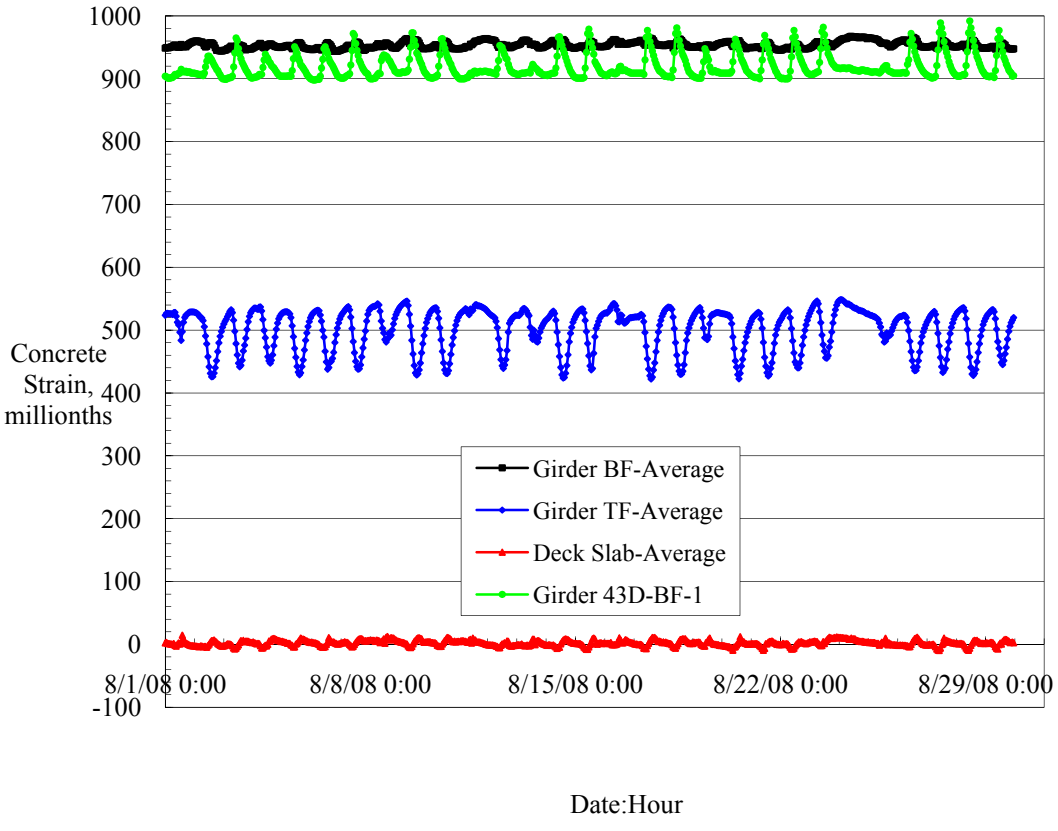

Figure 19
Measured concrete temperature data – August 2008

The vibrating wire strain gage located in the bottom flange of exterior Girder 43D on the south side of the bridge span (gage 43D-BF-1) registered daily concrete strain fluctuations of as much as 80 millionths as indicated by the green plot line in Figure 19. These strain fluctuations appear to follow the same trend as the concrete temperature fluctuations shown in Figure 18 and were likely accentuated by the effect of increased solar radiation on the southern bridge exposure throughout the year.

The daily strain fluctuations shown in Figure 19 for the month of August are driven by changes in weather conditions at the bridge site (temperature, cloud cover, precipitation, relative humidity, etc.). Although not sustained for prolonged periods of time, these fluctuations will still have a temporary superimposed effect on both girder and deck slab concrete stress levels. However, quantifying these weather-induced changes in stress levels is a very complex problem, requiring consideration of several parameters including non-linear temperature gradients, material properties, longitudinal continuity of the bridge span, and sources of restraint.

CONCLUSIONS

Design and construction of the Rigolets Pass Bridge has demonstrated yet again that a bridge using HPC can be successfully constructed in Louisiana using locally available materials. Specific conclusions from various aspects of the research are as follows:

1. The specified concrete compressive strength for the HPC girders was 6,670 psi (46 MPa) at release and 10,000 psi (69 MPa) at 56 days. The measured concrete compressive strengths for the four instrumented girders exceeded the specified strength at both the release and 56-day test ages.

2. The *AASHTO Standard Specifications for Highway Bridges* and *LRFD Bridge Design Specifications* equations for modulus of elasticity provided a conservative prediction of the actual measured girder concrete modulus of elasticity obtained from this research. However, based on data from other previous HPC research sponsored by LTRC, use of modulus of elasticity values that are slightly less than those predicted by the AASHTO expression may be warranted when specified concrete compressive strengths exceed 12,000 psi (83 MPa).

3. The *AASHTO Standard Specifications for Highway Bridges* and *LRFD Bridge Design Specifications* equations for modulus of rupture given in Article 9.15.2.3 and Article 5.4.2.6, respectively, provided a conservative prediction of the actual measured girder concrete modulus of rupture obtained from this research. Based on data from this research and other previous HPC research sponsored by LTRC, continued use of these equations within the context cited in the AASHTO standards appears warranted.

4. The average measured chloride permeability of the girder concrete obtained from this research (151 coulombs) was considerably less than the 2,000-coulomb limit stipulated in the project specifications. Based on the measured chloride permeability data generated from this research, and from the Charenton Canal Bridge research, the use of silica fume provides a much greater benefit relative to reducing overall permeability than Class C fly ash.

5. According to the ACI Committee 209 Report (ACI 209R-92), the ultimate creep coefficient of concrete is normally in the range of 1.30 to 4.15, and ultimate shrinkage is normally in the range of 415 to 1070 millionths *[8]*. The creep coefficient after one year reflected by the measure test data fell approximately in the middle of the expected range. The measured shrinkage after one year fell well below the expected

range. Based on these data, lower-than-normal measured girder prestress losses due to the combined effects of creep and shrinkage would be expected.

6. The specified concrete compressive strength for the deck slab concrete was 4,200 psi (29 MPa) at 28 days. The measured concrete compressive strengths for all test ages (7, 28, and 90 days) exceeded the specified strength.

7. The average measured chloride permeability of the deck slab concrete obtained from this research (1,028 coulombs) was less than the 2,000-coulomb limit stipulated in the specifications for the Rigolets Pass Bridge project.

8. Force levels measured in selected prestressing strands made just prior to release were approximately 8 percent less than the specified initial force level. Approximately half of this reduction in prestress force was evident immediately after stressing all of the strands. The balance of the reduction was likely caused by thermal expansion due to the heat generated by the concrete during initial curing.

9. Total average measured prestress loss for the four instrumented HPC girders was approximately 50 percent of the corresponding final values calculated using the provisions of the *AASHTO Standard Specifications for Highway Bridges*. Based on the measured long-term prestress loss data from this research, and from previous LTRC-sponsored HPC research, the provisions of the *AASHTO Standard Specifications for Highway Bridges* have consistently predicted prestress losses in high-strength concrete bridge girders that were greater than the actual measured losses.

10. Total average measured prestress loss for the four instrumented HPC girders was 65 to 87 percent of the corresponding final values calculated using the provisions of the *AASHTO LRFD Bridge Design Specifications*. Therefore, the *AASHTO LRFD Bridge Design Specifications* provided a better prediction of the actual measured prestress loss than the *AASHTO Standard Specifications for Highway Bridges*.

11. Based on the measured prestress losses from previous HPC research sponsored by LTRC, and results from this research, there is some evidence to suggest that the use of silica fume in the bridge girder concrete may provide a greater benefit with respect to reducing total prestress loss than Class C fly ash.

12. Girder deflections at various stages of construction were calculated using a traditional moment-area approach considering both design (as-designed) and measured (as-

constructed) properties. The as-designed calculated deflection values generally provided better correlation with corresponding measured values than the as-constructed calculated deflection values. However, it should be noted that neither of the calculated deflection scenarios accounted for the effects of prestress loss or shrinkage of the deck slab concrete. It is also significant to note that the girder deflection measurements were taken under a variety of different temperature and cloud cover conditions and, therefore, could have been influenced by subtle concrete temperature gradients within the bridge superstructure.

13. The measured deck strains exhibited a trend of initial compression (presumably due to initial drying shrinkage), followed by a gradual transition to increasing tension (likely due to the effects of girder creep and shrinkage deformations). Trends observed in the measured deck strains were consistent with corresponding trends observed in measured girder concrete strains and deflections.

14. Based on the trends and fluctuations of measured concrete strains documented during typical winter and summer exposure conditions, it is apparent that changing weather conditions at the bridge site will have an effect on in-service stress levels in both the girders and deck slab. However, quantifying these weather-induced changes in stress levels is a very complex problem, requiring consideration of several parameters including non-linear temperature gradients, material properties, longitudinal continuity of the bridge span, and source of restraint.

RECOMMENDATIONS

Based on the Discussion of Results and Conclusions reported herein, the following recommendations are offered for consideration:

1. LADOTD should continue implementing HPC with specified compressive strengths up to 10,000 psi (69 MPa) on all bridges where its use is beneficial and economical.

2. LADOTD should continue to use the existing AASTHO equations for modulus of elasticity and modulus of rupture when the specified girder concrete compressive strength is 12,000 psi (83 MPa) or less. When the specified girder concrete compressive strength exceeds 12,000 psi (83 MPa), the use of a slightly reduced value for the modulus of elasticity would be appropriate.

3. The use of HPC incorporating 10 percent silica fume by weight of cementitious materials should be considered whenever extremely low permeability is desirable or required.

4. LADOTD should continue implementation of research programs similar to this program on projects where HPC is specified in order to continue expansion of the existing material and performance database.

ACRONYMS, ABBREVIATIONS, AND SYMBOLS

AASHTO	American Association of State Highway and Transportation Officials
ACI	American Concrete Institute
ASTM	American Society for Testing and Materials
Ave	average
BF	bottom flange
BT	bulb tee
º C	degrees Celsius
Cyl.	cylinder
cu	cubic
DAS	data acquisition system
E_c	concrete modulus of elasticity
º F	degrees Fahrenheit
fl oz	fluid ounce
ft.	foot / feet
f'_c	specified compressive strength of concrete
f_r	concrete modulus of rupture
GCP	Gulf Coast Pre-Stress, Inc.
HPC	high-performance concrete
in.	inch(es)
kg	kilogram
kN	kilonewton
ksi	kips per square inch
K_1	correction factor for source of aggregate
LADOTD	Louisiana Department of Transportation and Development
L	liter(s)
LRFD	Load and Resistance Factor Design
LTRC	Louisiana Transportation Research Center
lb	pound(s)
MOR	modulus of rupture
MPa	megapascal

m	meter(s)
mm	millimeter(s)
N	newton
No.	number
PCI	Precast/Prestressed Concrete Institute
pcf	pounds per cubic foot
pp	pages
psi	pounds per square inch
sq	square
TF	top flange
VWSG	vibrating wire strain gage
w_c	unit weight of concrete
yd	yard
@	at
Δf_{pES}	loss in prestressing steel due to elastic shortening
Δ_{fpLT}	long term prestress loss due to concrete creep, concrete shrinkage and steel relaxation

REFERENCES

1. Bruce, R. N.; Russell, H. G.; Roller, J. J.; and Martin, B. T., "Feasibility Evaluation of Utilizing High Strength Concrete in Design and Construction of Highway Bridge Structures," Final Report – Louisiana Transportation Research Center, Research Report No. FHWA/LA-94-282, Baton Rouge, LA, 1994, 168 pp.

2. Bruce, R. N.; Russell, H. G.; Roller, J. J.; and Hassett, B. M., "Implementation of High Performance Concrete in Louisiana Bridges," Final Report – Louisiana Transportation Research Center, Research Report No. 310, Baton Rouge, LA, 2001, 67 pp.

3. Bruce, R. N.; Russell, H. G.; and Roller, J. J., "Fatigue and Shear Behavior of HPC Bulb-Tee Girders," Interim Report – Louisiana Transportation Research Center, Research Report No. FHWA/LA. 03/382, Baton Rouge, LA, 2003, 57 pp.

4. Bruce, R. N.; Russell, H. G.; and Roller, J. J., "Fatigue and Shear Behavior of HPC Bulb-Tee Girders," Final Report – Louisiana Transportation Research Center, Research Report No. FHWA/LA. 05/395, Baton Rouge, LA, 2005, 59 pp.

5. *Standard Specifications for Highway Bridges*, Sixteenth Edition, American Association of State Highway and Transportation Officials, Washington, DC, 1996.

6. Louisiana Standard Specifications for Roads and Bridges, State of Louisiana, Department of Transportation and Development, Baton Rouge, LA, 2006, 895 pp.

7. *AASHTO LRFD Bridge Design Specifications*, Fourth Edition (Including 2008 Interim), American Association of State Highway and Transportation Officials, Washington, DC, 2007.

8. ACI Committee 209, "Prediction of Creep, Shrinkage and Temperature Effects in Concrete Structures," (ACI 209R-92) (Reapproved 1997), American Concrete Institute, Detroit, 1992, 47 pp.

9. PCI Plant Certification Committee, “Manual for Quality Control for Plants and Production of Structural Precast Concrete Products,” MNL-116-99, Precast, Prestressed Concrete Institute, Chicago, IL, 1999.

10. PCI Committee on Prestress Losses, “Recommendations for Estimating Prestress Losses,” *PCI Journal*, Vol. 20, No. 4, July-August 1975, pp. 44-75.